

Hochschule Osnabrück
University of Applied Sciences

Fakultät Ingenieurwissenschaften und Informatik

Masterarbeit

über das Thema

**Start-up and investigation of a solar panel test
plant with PV tracker**

Vorgelegt durch

Sandra Pascual Retuerta

Matrikelnummer: 737100

Erstprüfer/in (Themensteller/in): Prof. Dr. Sandra Rosenberger
Zweitprüfer/in: Mr. Stefan Höcker

Ausgabedatum: 04.07.2016

Abgabedatum: 07.07.2016

DECLARATION CERTIFIED OF WORKING ALONE

I hereby declare that I own this work and have made it independently without using any help; and that the concepts acquired directly or indirectly from other sources are identified as such. The work has never been presented in the same or similar form to another examination board and has not been published yet.

Ich erkläre hiermit an Eides Statt, dass ich die vorliegende Arbeit selbständig und ohne Benutzung anderer als der angegebenen Hilfsmittel angefertigt habe; die aus fremden Quellen direkt oder indirekt übernommenen Gedanken sind als solche kenntlich gemacht. Die Arbeit wurde bisher in gleicher oder ähnlicher Form keiner anderen Prüfungsbehörde vorgelegt und auch noch nicht veröffentlicht.

ACKNOWLEDGEMENTS

I would like to thank my family for all the support during the past years and for allowing me to study what I wanted and to come to Germany, because nothing of this would have been possible without them. I would also like to thank my classmates and friends for all the help during the Bachelor and Master, this was a truly team race. Especially I would like to thank my best friend Miriam for being there with me along the whole path for the past 20 years, always supportive and without any complaint in my bad moments. Moreover, in particular, I want to thank Jonatan, for helping me and trying to cheer me up in the most stressful moments and when I wanted to give up. This thesis would not exist without you.

Furthermore, thanks to Pablo Sanchis for his entire disposition answering to all of my doubts during all the Erasmus process, he has made this much easier. Besides, I need to thank my colleagues from the SE and SD buildings for being so kind and trying to integrate me in their department, always making me feel welcomed. Finally, I would like to thank to Prof. Dr. Sandra Rosenberger and to Mister Stefan Höcker for their incalculable help, since they have accompanied me through the entire research and helped me to solve all the problems and obstacles I found on the way.

ABSTRACT IN ENGLISH

The topic of this thesis is the investigation about solar panels. On the practical side, a circuit was designed in order to measure the most important magnitudes when working with solar panels: the voltage, the current, the temperature, the radiation and the angle. This will allow the user to know how to reach the best conditions to generate solar energy. Furthermore, the voltage and the current are necessary to draw the characteristic P-V curve of the panel and thus find the maximum power that it is possible to get.

On the theoretical side, an investigation about the spectrum of the light and its effects in the characterization of a solar panel was carried out. As the weather in Germany is usually not sunny, it is necessary to work with halogen lights sometimes. It is then very important to know how to work properly with these lights and get valid results.

ABSTRACT IN GERMAN

Thema der Arbeit ist der Aufbau und die Inbetriebnahme einer Solaranlage. Der Praktische Teil beinhaltet die Entwicklung einer Schaltung zur Erfassung der relevantesten Messgrößen, die beim Betrieb eines Photovoltaikmodules anfallen: Spannung, Strom, Temperatur, Einstrahlleistung und Modulneigungswinkel. Diese Messwerte bilden die Grundlage für eine optimale Energiegewinnung. Des Weiteren ist eine Spannungs- und Strommessung notwendig, damit eine PV-Kennlinie erstellt werden kann, um ein Modul im MPP zu betreiben.

Der Theoretische Teil der Arbeit befasst sich mit dem Spektrum des Lichtes und welchen Einfluss dieser auf den Photoeffekt ausübt. Bei der Verwendung von Halogenlicht anstelle von Natürlichem Sonnenlichtes entstehen Abweichungen, die betrachtet werden, um korrekte Ergebnisse zu erhalten.

INDEX

1.	INTRODUCTION AND OBJECTIVES	17
2.	SOLAR ENERGY	18
2.1.	Solar energy in the world	18
2.2.	Solar energy in Germany	19
2.3.	Photovoltaic solar panel	20
3.	INFLUENCE OF THE SPECTRUM OF THE LIGHT	23
3.1.	Spectrum of the light: definition	23
3.2.	Characterization of a solar panel	24
3.3.	Influence of the spectrum of the light in the characterization of solar panels	25
3.3.1.	Analysis of different light sources	26
3.3.2.	Theoretical analysis of the halogen lamps	28
3.3.3.	Recommendations	31
3.4.	Influence of the spectrum of the light in the solar cell degradation	32
4.	START-UP	34
4.1.	Hardware and software	34
4.1.1.	LabVIEW™	34
4.1.2.	Software problems	36
4.1.3.	NI myRIO™	37
4.1.4.	Arduino™	38
4.2.	Voltage measurement	40
4.3.	Temperature measurement	41

4.3.1.	1-Wire® protocol	42
4.3.2.	Sensor DS18B20	43
4.3.3.	Application	44
4.4.	Angle measurement	44
4.4.1.	Protocol I ² C	45
4.4.2.	Magnetometer Melexis MLX90393 Triaxis® Micropower Magnetometers	46
4.4.3.	Application	48
4.5.	Radiation measurement	49
4.5.1.	Sensor GBS01	49
4.5.2.	Application	50
4.6.	Current measurement	51
4.6.1.	Process	51
4.6.2.	Allegro™ ACS712	52
4.6.3.	Application	53
4.7.	Saving data	54
4.8.	Final application	56
4.8.1.	In Arduino™	57
4.8.2.	In LabVIEW™	60
4.8.3.	Physical circuit	66
4.9.	Manual of the program for the final user	68
5.	RESULTS	72
5.1.	Measurement 1	72

5.2.	Measurement 2	72
5.3.	Measurement 3	73
5.4.	Measurement 4	73
5.5.	Measurement 5	73
5.6.	Measurement 6	73
5.7.	Measurement 7	74
5.8.	Measurement 8	75
5.9.	Measurement 9	76
5.10.	Measurement 10	76
5.11.	Measurement 11	77
5.12.	Measurement 12	77
5.13.	Measurement 13	78
5.14.	Measurement 14	78
6.	CONCLUSION	79
7.	DISCUSSION OF THE RESULTS	80
8.	SUMMARY AND PERSPECTIVES	81
9.	BIBLIOGRAPHY	82
10.	APPENDIXES	84
10.1.	Appendix 1: Results measurement 1	84
10.2.	Appendix 2: Results measurement 2	86
10.3.	Appendix 3: Results measurement 3	87
10.4.	Appendix 4: Results measurement 4	88

10.5.	Appendix 5: Results measurement 5	89
10.6.	Appendix 6: Results measurement 6	91
10.7.	Appendix 7: Results measurement 7	92
10.8.	Appendix 8: Results measurement 8	93
10.9.	Appendix 9: Results measurement 9	94
10.10.	Appendix 10: Results measurement 10	95
10.11.	Appendix 11: Results measurement 11	97
10.12.	Appendix 12: Results measurement 12	98
10.13.	Appendix 13: Results measurement 13	99
10.14.	Appendix 14: Results measurement 14	102

LIST OF FIGURES

Fig. 2.1 Solar PV World Record (Germany 2012)	19
Fig. 2.2 Differences between a polycrystalline and a monocrystalline solar cell	21
Fig. 2.3 Kyocera KC60 module used in the experiments of the thesis	22
Fig. 3.1 Spectrum of the light	23
Fig. 3.2 Characteristic I-V curve of a solar panel	25
Fig. 3.3 Relative output of the different PV solar cells under different lighting conditions, compared to the spectrum of the Sun. Source: A Proposal for Typical Artificial Light Sources for the Characterization of Indoor Photovoltaic Applications (see section 9)	28
Fig. 3.4 Tungsten halogen lamp spectral distribution at different temperatures	30
Fig. 3.5 Comparison of light soaked c-Si solar cell I-V characteristics under different filters (light intensity: 1 kW/m ² , duration: 10h, temperature: 25°C). Source: Effectiveness of full spectrum light soaking on solar cell degradation analysis (see section 9).....	33
Fig. 4.1 Example of LabVIEW™ front panel	35
Fig. 4.2 Example of LabVIEW™ block diagram	35
Fig. 4.3 NI myRIO	37
Fig. 4.4 Arduino UNO board	39
Fig. 4.5 Arduino™ Nano board	40
Fig. 4.6 Circuit for the voltage measurement	41
Fig. 4.7 Communication between the master and the slave in 1-Wire protocol.....	42
Fig. 4.8 Temperature sensor DS18B20.....	43
Fig. 4.9 Circuit of the temperature measurement	44
Fig. 4.10 Communication between master and slave in I ² C protocol	45

Fig. 4.11 Magnetometer Melexis MLX90393	46
Fig. 4.12 Schematic of MLX90393 and different addresses	47
Fig. 4.13 Circuit of the angle measurement	48
Fig. 4.14 Radiation sensor GBS01.....	50
Fig. 4.15 Circuit of the radiation measurement	51
Fig. 4.16 Current sensor Allegro™ ACS712.....	53
Fig. 4.17 Circuit of the current measurement.....	54
Fig. 4.18 Example of an Excel sheet	55
Fig. 4.19 Example of an empty Notepad file	55
Fig. 4.20 Summary of the protocols and connections.....	56
Fig. 4.21 Part 1 of the LabVIEW™ program (settings of the serial port)	61
Fig. 4.22 Part 2 of the LabVIEW™ program (separation of the variables).....	62
Fig. 4.23 Part 3 of the LabVIEW™ program (conversion of the voltage).....	63
Fig. 4.24 Part 3 of the LabVIEW™ program (conversion of the radiation)	64
Fig. 4.25 Relation between the radiation and the output value of the sensor BGS01	64
Fig. 4.26 Part 5 of the LabVIEW™ program (conversion of angles, current and temperature) ..	65
Fig. 4.27 Part 6 of the LabVIEW™ program (saving the data into a TXT file)	66
Fig. 4.28 Circuit welded (version with silver wire as shunt resistor).....	67
Fig. 4.29 Final assembly.....	68
Fig. 4.30 Display with the time between samples (modifiable by the user).....	68
Fig. 4.31 Display to select the TXT file where the data will be saved	69
Fig. 4.32 Display where the user must select the Arduino™ port.....	69

Fig. 4.33 Displays with the results of the measurements (left side of the front panel).....	70
Fig. 4.34 Displays with variables to check the correct performance of the program (right side of the front panel)	70
Fig. 4.35 Stop button (bottom of the front panel).	71
Fig. 5.1 Graphic created in Microsoft Excel® showing the results of Measurement 6	74
Fig. 5.2 Graphic created in Microsoft Excel® showing the results of Measurement 7	75
Fig. 5.3 Graphic created in Microsoft Excel® showing the results of Measurement 8	75
Fig. 5.4 Graphic created in Microsoft Excel® showing the results of Measurement 9	76
Fig. 5.5 Graphic created in Microsoft Excel® showing the results of Measurement 11	77

1. INTRODUCTION AND OBJECTIVES

The photovoltaic solar energy has grown during the past years, and now it is one of the most important renewable energies in the world. One of the main reasons for this is that the use of photovoltaic solar energy is a good method to provide electricity to isolated environments. This is especially vital for developing countries, because installing photovoltaic modules they would be able to have electricity in spite of the lack of a good electrical network. Another reason is that it is one of the easiest methods to create energetically self-sufficient buildings. This is very important, and especially in Germany, thanks to the effort that the government has put into the development of renewable energies. That is why Germany is one of the top countries in photovoltaic solar energy and in renewable energies.

In view of all this facts, it is essential to teach about the photovoltaic solar energy because it will become more important over the years, due to the plan of German government to cover all the energetic demand with renewable energies before 2050. Thus, the universities and in particular Hochschule Osnabrück have included the photovoltaic solar energy as an important part of the education of future engineers.

In order to teach about this energy, some practical lessons will be hold. In those lectures, the students will learn about the photovoltaic energy and the influence that external parameters can have in the production of electricity. To facilitate this learning, an application to measure the different characteristics and draw the V-I curve of a solar panel was programed. The corresponding circuit with the necessary sensors was created. The objectives of this thesis are the following:

- Design and create a program to measure the most important characteristics of a solar panel, so the students can modify them and learn about the influence of external parameters in the electrical production.
- Investigate about the spectrum of the light and its effect in the generation of photovoltaic energy, as well as in the degeneration of solar cells.

2. SOLAR ENERGY

The photovoltaic solar energy is a source of energy that produces electricity of renewable origin, directly obtained through the solar radiation thanks to a semiconductor device called photovoltaic cell. This type of energy is used to produce innumerable applications and autonomous devices, to provide energy to buildings isolated from the electric network, and to produce renewable energy at large scale. Due to the growing demand of renewable energy, the production of solar cells and photovoltaic installations has considerably developed during the past years. Thanks to this fact, the solar photovoltaic energy has become the third most important renewable energy source (in terms of capacity installed), after hydroelectric and wind power.

With the latest progress, the cost of photovoltaic solar energy has been reduced since the first commercial solar cells were produced, increasing the efficiency at the same time, and achieving a competitive cost of the electric generation, similar to the conventional energy sources. Moreover, the useful life of the solar cells has augmented to approximately 30 years.

2.1. Solar energy in the world

The photovoltaic solar energy has been rising in an exponential curve for the past 20 years, motivated by the new challenges in energy generation. During this period, it has evolved from a market based in small-scale applications to become a conventional source of electricity. Historically, EEUU has led the installation of photovoltaic energy since its origin to 1996, where the installed capacity reached 77 MW, more than any other country up to that date. Afterwards it was surpassed by Japan, which maintained the top position until Germany surpassed it in 2005. In the beginning of 2016, Germany was approaching to 40 GW installed. However, China, one of the countries where the photovoltaic energy is experimenting the most vertiginous increase, exceeded Germany and became from then the greatest producer of photovoltaic energy in the world. It is expected that China will multiply its installed power and will achieve 150 GW in 2020.

When the photovoltaic systems were first recognized as a promising technology or the production of renewable energy, different countries started to implement subsidies to provide of economic incentive to the investors. As a consequence of the development, the cost of the photovoltaic energy has significantly decreased. The most important factors have been the technological improvements and the scale economies, especially when the production of solar modules and cells rose uncontrollably in China.

2.2. Solar energy in Germany

In the beginning of 2016, Germany had nearly 40 GW of photovoltaic solar power installed. The photovoltaic market has grown considerably since the beginning of the XXI century thanks to the creation of a regulated tariff to the production of renewable energy, introduced for the “German Renewable Energy Act”, a law published in 2000. Since then, the cost of the photovoltaic installations decreased more than 50% in 5 years (2006-2011). Germany has settled the objective of producing the 35% of energy with renewable sources by 2020, and the 100% in 2050.

Germany has achieved several records in photovoltaic energy during the last years. In two consecutive days in May 2012, the photovoltaic systems installed in the country produced 22000 MW/h at midday (Fig. 2.1) , which is equivalent to the power of 20 nuclear plants working at full capacity. Then the 21st July 2013 Germany reached 24 GW also at midday. In June 2014 Germany broke another record when they covered the 50,6% of the electric demand of the day with photovoltaic energy.



Fig. 2.1 Solar PV World Record (Germany 2012)

Since the government is conscious that the energy storage is essential for the massive installation of renewable systems due to the intermittence of those sources, the 1st May 2013 Germany started a new program of subsidies to encourage photovoltaic systems with storage batteries. With this method it is possible to dispose of renewable energy even when the resource is not available (at night for example), and it helps to the stability of the electrical system.

The German model is characterised for the strong presence of small installations, which has many advantages due to the smaller loss in transportation. The cause of this model is the German legislation, which offers bigger advantages to small installations. Approximately the 90% of the solar panels installed in Germany are located over roofs. For example, the record achieved in 2013 was possible thanks to 1,3-1,4 millions of small photovoltaic systems.

This model has been encouraged with the newest version of the “German Renewable Energy Act”. According to this law, new buildings must be efficient and produce by renewable sources a percent of the consumed energy. Therefore, many buildings have now solar panels in the roof to generate power, especially for heating system.

2.3. Photovoltaic solar panel

A solar panel is a device that captures energy from solar radiation for its exploitation. A photovoltaic solar panel is formed by numerous cells that transform light into electricity. Those cells are sometimes called photovoltaic cellules. The cells generate energy due to the photovoltaic effect. The photovoltaic effect is a process where light energy produces positive and negative charge in two near semiconductors of different type. It creates then an electric field that is capable of generating a current.

The most common material for solar cells are crystalline silicon. The most used silicon cells in photovoltaic panels are three:

- Monocrystalline silicon cells: formed by only one silicon crystal. They present a uniform dark blue colour.
- Polycrystalline silicon cells: formed by an assembly of silicon crystals, which explains why their performance is worse than the monocrystalline ones. One characteristic is their colour, which is a more intense blue. The different colours can be seen in Fig. 2.2.
- Amorphous silicon cells: less efficient than the two others but also cheaper. They are used in small applications like watches or calculators.

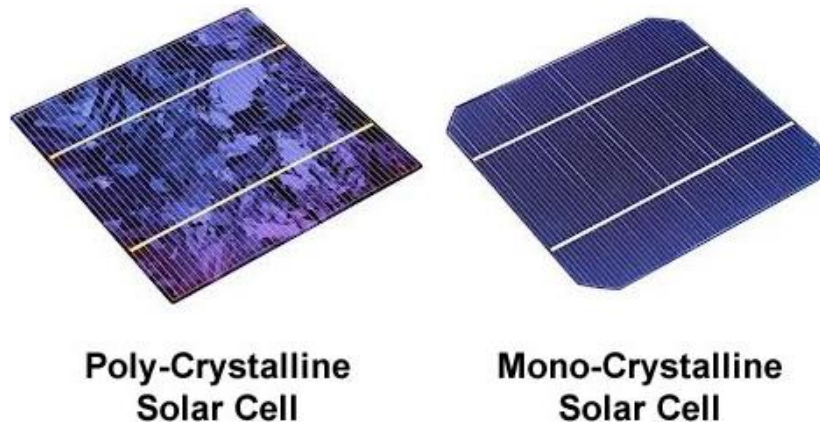


Fig. 2.2 Differences between a polycrystalline and a monocrystalline solar cell

The bigger the crystals are, the greater the effectivity is; but also the weight, thickness, and cost of the panel. The performance of monocrystalline cells can reach 22%, while amorphous cells performance can be below 10%, but they are much lighter and cheaper. The cost of the solar panels has decreased since the first commercial solar cells were made, and now the average cost of electric generation is competitive with conventional energy sources.

The fabrication process of a solar cell is complex. The crystalline ingots are cut in thin discs and then are polished to avoid possible damages caused by the cutting. Afterwards, some doping substances are added in the discs. Those doping substances are contaminants added to modify the conductive properties. The next step is the deposition of metallic conductors in each surface: a thin grid in the side that will face the sun, and a flat blade in the other. The solar panels are constructed attaching those cells in the appropriate way. To protect them from damages caused by radiation or for the normal functioning, they are covered by a glass in the frontal surface and they are glued on a substrate (a rigid panel or a soft blanket). Electric connections to fix the total output voltage are made, both parallel and serial. The glue and the substrate must be thermal conductors, because the cells get heated when absorbing the infrared energy that cannot be converted into electricity. That heat should be minimized as much as possible because it reduces the efficacy of the conversion. The assembly created with this process is a solar panel.

The structures to fix the solar panels are generally made of aluminium with stainless steel screws, to assure lightness and durability. The size of the structure is standard for surface, orientation and inclination (both horizontal and vertically).

The solar panel used is the Kyocera KC60 (Fig. 2.3), which is a multicrystal photovoltaic module. The efficiency of this module is over 14%, which is enough for the educational purposes of this work. Moreover, the module has a tempered glass cover and an EVA protective layer with PVF

back sheet, in order to proportion a good protection against the environmental conditions; although this is not so essential because the using of this module in the Hochschule Osnabrück is mainly indoors. Furthermore, it is laminated with an anodized aluminium frame to ease the installation and provide structural strength.

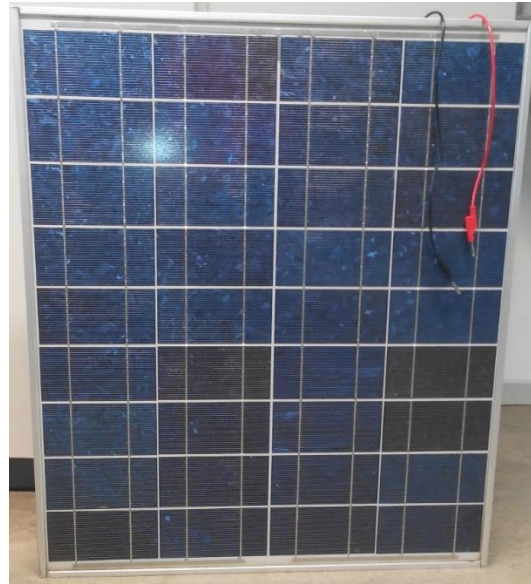


Fig. 2.3 Kyocera KC60 module used in the experiments of the thesis

The maximum power it can provide is 60 W and the open circuit voltage is 21,5 V. The short-circuit current is 3,73 A which is rather high so it is important to be careful when using it because the wrong manipulation of this panel can be dangerous. The measures are 751x652x54 mm, that means it is big enough to provide with energy in order to test the different characteristics for the application, but it is also small enough to ease its manipulation. Another advantage is that it only weights 6kg, so it is simple to transport it outside and inside the laboratory.

In spite of using one single panel to perform the experiments narrated in this work, there are more possibilities by uniting more modules. In the Hochschule Osnabrück there is an aluminium structure that contains 3 KC60 panels and a monocrystalline panel. This structure incorporates two PV tracker in two sides, in order to create a more efficient following system. Thanks to those PV trackers, the module positions itself to face the brightest point in the sky, so it can avoid shadows and follows the sun during the different seasons and times of the day. This following is automatic, although the module can also be controlled with a joystick.

3. INFLUENCE OF THE SPECTRUM OF THE LIGHT

3.1. Spectrum of the light: definition

The electromagnetic spectrum is the energetic distribution of the electromagnetic waves. Referring to an object it is called electromagnetic spectrum or just *spectrum* to the electromagnetic radiation that it emits (emission spectrum) or that it absorbs (absorption spectrum). This radiation allows the identification of the object. The spectrum can be observed through a spectrometer, and this device can perform measurements like the wavelength, frequency and intensity of the radiation.

The electromagnetic spectrum extends from the radiation with a lower wavelength as gamma rays or X rays, going through the ultraviolet light and visible light, to the waves with higher wavelength as radio waves. Formally, the spectrum is infinite and continuous, although it is said that the minimum wavelength possible would be the Planck length, and the maximum would be the universe size itself. A representation of this spectrum can be seen in Fig. 3.1.

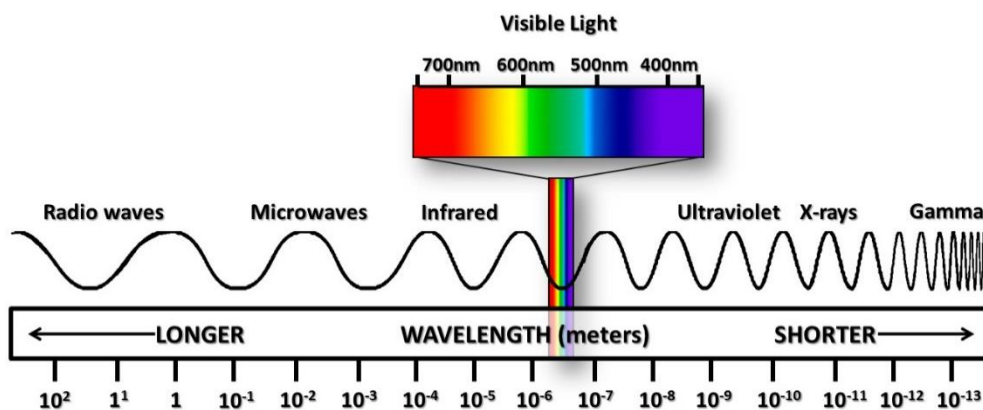


Fig. 3.1 Spectrum of the light

According to their wavelength, the spectrum is divided in regions. In this case, the most important range is the visible spectrum. The visible spectrum is commonly called light, and it is a special type of radiation with a wavelength between 380 nm and 780 nm depending on the eye. The sun and similar stars emit most part of their radiation in this range. Moreover, it is the only region that the human eye can perceive; although not all the eyes have the same precision and therefore every person can distinguish a different spectrum.

3.2. Characterization of a solar panel

A critical aspect of the photovoltaic systems is the electric characterization of the photovoltaic technology that is being used. In order to design the power electronics that are necessary to test a PV module, it is essential to model the electrical characteristics. This information is necessary to measure and estimate the energy that a photovoltaic installation will produce. Moreover, the electric characterization is a fundamental part for the development of new prototypes of solar cells.

The results of this characterization are the short-circuit current, the open-circuit voltage, the maximum power generated and the conversion efficiency; but all of them are influenced by solar radiation, temperature, and load impedance. Therefore, these parameters are necessary in order to try to characterise the panel under the most stable conditions. Those results are usually reported in the data sheet of the commercial photovoltaic modules, but the main disadvantage is that the parameters are not all mentioned, so it is impossible to know the conditions of the characterization.

Usually, in the data sheet of the modules the characteristic curve is also drawn. The characteristic curve (or V-I curve), represents the voltage in the terminals of the panel and the current provided by it, measured under determined conditions of isolation and temperature. Modifying the external load from zero to infinite, several pairs of values (V-I) can be measured, and the interpolation of all of them provides the characteristic curve. The open circuit voltage (V_{oc}) is measured when no load is connected to the circuit, and in that point the current will be zero because the circuit is open. On the other side, when the terminals of the cell are short-circuit, the voltage is zero but the current is maximum, which is the short-circuit current (I_{sc}). Other two interesting points are the V_{mp} ($\approx 0,8-0,9 V_{oc}$) and the I_{mp} ($\approx 0,85-0,95 I_{sc}$), because the multiplication of those two values provides the maximum power point. An example of this curve is showed in Fig. 3.2.

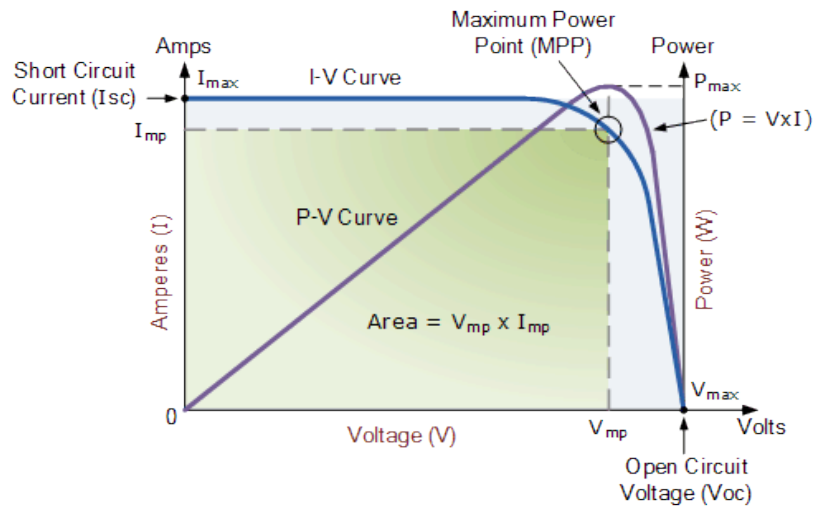


Fig. 3.2 Characteristic I-V curve of a solar panel

This characterization of the photovoltaic generators has to be done in an experimental way, due to the difficulty of modelling its electrical behaviour. A photovoltaic device has non-linear electric voltage-current characteristics that depend (also in a non-linear way) of ambient variables such as temperature and solar radiation. Furthermore, each photovoltaic technology has different responses for these ambient conditions. However, some mathematical models can help to this characterization even though they are not perfect because of the mentioned problems.

Because of all these reasons, photovoltaic devices need a reliable methodology of characterization that makes possible:

- Predict the energy generation of the device for a fixed conditions.
 - Compare the energetic performance of different photovoltaic technologies.
- Obtain models that allow the optimization of the energy extraction of the photovoltaic device and the electronic circuits associated to it.

3.3. Influence of the spectrum of the light in the characterization of solar panels

The reliability of the photovoltaic device characterization depends also of the light source used in its excitation. There are several international standards that detail how the optic characteristics of this light source should be, such as the IEC 60904-9 (International Electrotechnical Commission), the ASTM E927 (ASTM International) or the JIS C 8912 (Japanese Industrial Standards). As general conditions, the light source should have:

- Light spectrum similar to the Sun
- Constant light intensity

Nevertheless, it is difficult to find the perfect sun simulator in order to execute this characterization indoors. Typically, the light intensity of the sun is in a range between 100 and 1000 W/m², while in an office or factory this intensity is nearly 0, depending on the type of light source and the distance to the sensor. Furthermore, the spectrum of the artificial lights can be completely different from the spectrum of the Sun; because the spectrum not only depends on the source, but also on the presence of the reflected and diffused radiation.

In order to find out which light source is the best for the indoor characterization, a simulation with typical artificial light sources and diverse types of solar cells was executed. However, only the results for the polycrystalline cells will be highlighted because those are the cells used in the practical part of this work.

The radiation inside a building depends on the present light sources, but also on many other factors. For example, if there are some windows then the direct and diffuse sunlight can enter in the room through them, and the glass properties can affect to the spectrum of this sunlight. Furthermore, the location of the solar cell, its orientation or obstacles can alter the effectivity. Moreover, illuminated objects can absorb radiant energy and emit it at a different wavelength. However all those problems were not taken into account because the focus was the influence of the light source.

3.3.1. Analysis of different light sources

Firstly, the incandescent light is being analysed. An incandescent lamp is a glass balloon containing a filament that is heated to very high temperatures thanks to the Joule effect. For practical purposes, this filament can be considered as a black body with a temperature of 2856K, as said in a standard of the CIE (International Commission on Illumination). In order to properly compare different light sources all the sources must be scaled to an equal illumination, and in this case a value of 500 lux was chosen because it is the recommended illumination for offices. Despite of this, the value itself is not important, but the essential fact is that it has to be equal for all the sources.

Secondly, the halogen lamp will be analysed because its use is very extended. A halogen lamp is also a balloon with a filament, but the balloon is filled with gas in order to increase the lifetime

Chapter 3: Influence of the spectrum of the light

of the filament. Nevertheless, the temperature of the filament is similar as for an incandescent lamp. Therefore, it is possible to approximate a halogen lamp to the same black body.

Now the fluorescent tubes will be considered, which are also defined by a standard of the CIE. Fluorescent tubes are gas-discharge lamps that contain mercury vapour and use electricity to excite it. Those excited atoms produce ultraviolet light that provokes a phosphor to fluoresce, and consequently produce visible light. There are twelve types of fluorescent tubes, named F1 to F12. But according to the CIE, the types F2, F7 and F11 must be prioritized. F2 is a cool white fluorescent lamp with a temperature of 4230 K. F7 is a broad-band fluorescent lamp of 6500 K and F11 is a narrow tri-band fluorescent lamp with 4000 K.

The next light source taken into account is a high-pressure discharge lamp, in particular the pressure sodium lamp, which utilizes sodium in an excited state to produce light. In spite of the existence of low-pressure and high-pressure sodium lamp, the high-pressure one was used because of its broader spectrum. Another high-pressure discharge lamp with a broad spectrum is the metal halide lamp, which produces light using an electric arc in a gaseous mixture of vaporized mercury and metal halides. Those two light sources are also determined by a CIE standard.

The last light source considered for the experiment is the **Light Emitting Diode (LED)**, which is a solid-state lamp that emits light thanks to the electroluminescence of a bandgap material. The technology of this light source is currently improving, so there is not a standard yet.

In order to check the best light sources, the electrical output of the solar cell was calculated and compared to the output of that same solar cell outdoor with the standard spectrum of the sunlight. Then it was confirmed that the black body (incandescent or halogen lamps) is by far the best artificial light source for the photovoltaic energy generation. Nevertheless, halogen lamps are cheaper and more efficient than incandescent lamps, and that is why this source is the focus of the investigation. These results are shown in Fig. 3.3.

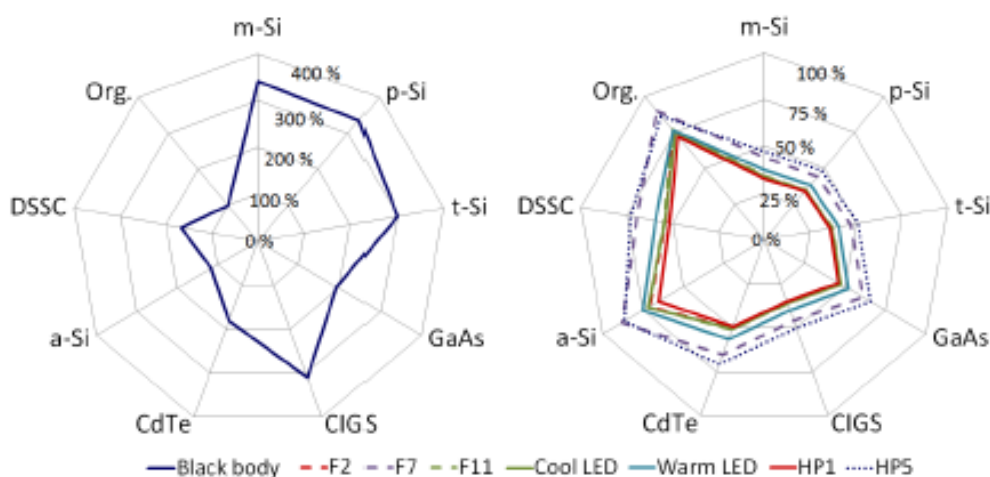


Fig. 3.3 Relative output of the different PV solar cells under different lighting conditions, compared to the spectrum of the Sun. Source: A Proposal for Typical Artificial Light Sources for the Characterization of Indoor Photovoltaic Applications (see section 9)

3.3.2. Theoretical analysis of the halogen lamps

The energy emission due to the heat contained in the emitting body is known as thermal radiation. The incandescence phenomenon comprise only the thermal radiation with energy in light form. So, only the one whose frequency is between the limits of the visible spectrum. In the group of incandescent objects that are used as a light source, the electric incandescent lamps can be found. They have a resistive filament that heats after an electric current pass. There are different categories of electric incandescent lamps, and the ones with better performance are halogen lamps.

Halogen lamps have a tungsten filament, encapsulated in a glass filled with inert gas, usually a halogen gas like iodine or bromine. Tungsten and quartz are used as a resistive filament and encapsulated glass (respectively) because of their tolerance to very high temperatures without mechanical damage. When the filament reaches the highest temperature, the tungsten of the filament starts to evaporate. The atoms of the tungsten, in gas form, react with the halogen gas and create another gas called halide. This new gas tends to return to the centre of the lamp, where the deteriorated filament is. As the halide is an unstable gas, when its molecules are directly exposed to the heat of the filament, they split again in metallic tungsten, which deposits in the filament, reconstructing it. This process allows the filament to recycle and last much more. Moreover, the gas avoids the deposit of the evaporated filament in the intern walls of the glass, which is an advantage because this would make the glass darker and the brightness would be reduced.

Chapter 3: Influence of the spectrum of the light

There are three properties of the halogen light sources that must be considered when characterizing photovoltaic devices. The first one is the electromagnetic spectrum. The spectral irradiance generated by the tungsten filament depends mainly of its temperature and the emissivity coefficient (ϵ). The emissivity coefficient is not constant, but it changes with the temperature and the spectral frequency. However, for the operation temperature and the spectral frequency range for the solar cells, it can be considered as a constant. Moreover, it is possible to approximate the spectral irradiance of the tungsten lamps to the spectral irradiance of a black body ($\epsilon=1$). A black body is an ideal object that can absorb all the energy that have an impact on its surface from the exterior and can emit all the energy that impacts from its interior. Furthermore, the solar spectrum approximates to a black body spectrum with a temperature of 5778 K.

The spectral irradiance of a black body is determined by:

$$I(\nu, T) = \frac{2h\nu^3}{c^2} \frac{1}{e^{h\nu/kT} - 1} \quad \text{Equation 1}$$

I: spectral irradiance of a black body

T: temperature of the body

ν : frequency

c: light velocity

h: Planck constant

k: Boltzmann constant

With this expression it is possible to obtain the curves of spectral irradiance of lamps of a black body at the typical temperatures of a halogen light. These curves are very similar to the curves of a halogen lamp, which appear in Fig. 3.4.

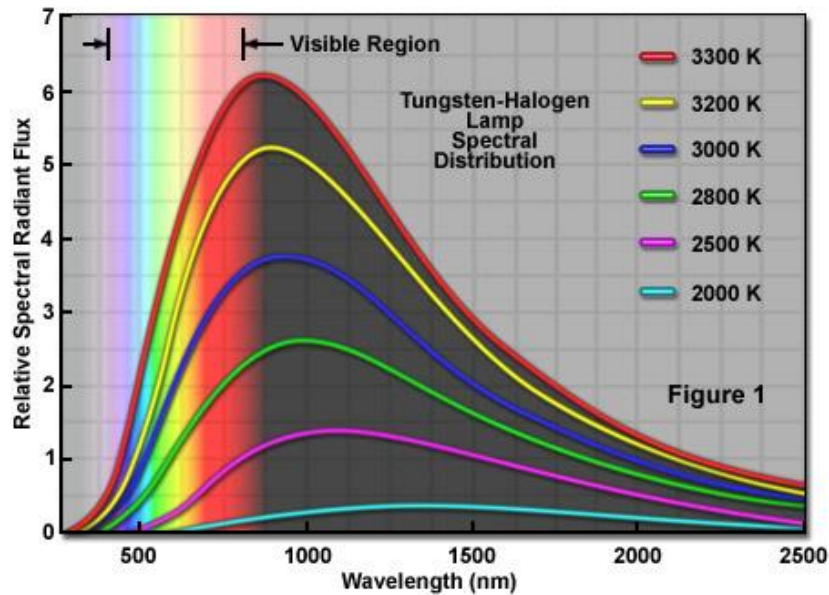


Fig. 3.4 Tungsten halogen lamp spectral distribution at different temperatures

With these curves it is possible to observe that the lamps emit energy in a wide range of the electromagnetic spectrum. However, photovoltaic devices generate current only in a limited range of the spectrum. The quantic energy indicates the current amount that a cell produces when it is irradiated by photons of a determined wavelength. The range of absorption is defined as the range of the electromagnetic spectrum in which the quantic efficiency is over 60%.

The higher the temperature, the more irradiance in the interesting wavelengths. However, there will always exist a percentage quite big of the spectral irradiance that will not generate electric current. This fraction of the spectrum will be dissipated as heat, which creates non-desirable effects for the characterization.

The second property that must be taken in consideration is the stability of the irradiance. The electric characterization must be done under constant irradiance. Two factors can affect the irradiance of the halogen light sources: the electronic circuit that energetically feeds the lamp, and the thermal transitory of the incandescent phenomenon.

There is a correlation between power dissipated by a filament and its temperature. Nevertheless, the temperature of a filament determines its spectral irradiance. The mathematical expression that relates electric power and temperature is:

$$\frac{v^2}{R} = K \cdot (T - T_0) + \varepsilon\sigma(T^4 - T_0^4)$$

Equation 2

Chapter 3: Influence of the spectrum of the light

v: voltage in the terminals of the filament

R: resistivity of the filament

K: constant that depends of the material of the filament

T: temperature

ϵ : emissivity

σ : Boltzmann constant

T_0 : ambient temperature

This implies that changes in the consumed power can also imply changes in the incandescence phenomenon. Therefore, it is necessary to supply constant voltage to the lamp to avoid possible variations in its light intensity. As most of the halogen lamps are prepared to work with alternate current, which can notably affect to the electric characteristics of the photovoltaic device, the experiments must be carefully performed.

On the other hand, a tungsten filament presents a dynamic in its temperature when there are changes in its feeding power. Therefore, the filament will experiment a transitory every time that there is a change in the electrical power, for example, during the start period.

The last property of the halogen light sources that must be considered is the heat transfer. Almost 85% of the energy emitted by a halogen lamp is inside or near the infrared, while only the 15-20% of the energy is emitted in the visible. Only 1% of the energy belongs to the ultraviolet range, and this energy is partially absorbed by the glass of the lamp. This way, a great part of the light spectrum that comes from this infrared energy is absorbed by the adjacent material and is transformed into heat. During the characterization process, this phenomenon can produce variations in the temperature of the cell, depending on the distance between the filament and the photovoltaic generator, the irradiance time and the temperature of the halogen lamp.

3.3.3. Recommendations

There are many disadvantages when a AC current is used to feed the halogen lamp in photovoltaic devices characterization, because the curve has many deformations that prevent

from knowing the real behavior of the panel. However, the stability of the light intensity that is achieved with DC current allows getting a characteristic curve without deformation.

It is easy to prove that the halogen light source are not a reliable source for the characterization of photovoltaic devices when there are variations in the feeding voltage, because this will cause variations in the temperature, intensity and distribution of the spectrum emitted by the filament.

Recommendations:

- Use DC current while feeding the lamp, to guarantee the stability in the light intensity.
- Use the halogen source in its point of maximum power dissipation, to rise its temperature and put its spectral distribution closer to the visible light, reduce the heat transfer and achieve a better simulation of the solar spectrum.
- Make the characterization after the transitory start period of the filament, in order to assure the stability of the radiation.
- While extracting the curve, try to expose the device to the halogen source the less time that is possible, in order to reduce the heating of the cell.

3.4. Influence of the spectrum of the light in the solar cell degradation

Since the photovoltaic energy is still experimenting a development process, there are many efforts to augment the conversion efficiency of the solar cells. However, the reliability and degradation of those solar cells is also an essential part of the improvement of this technology. Nevertheless, there are no standards to evaluate the solar cell degradation, due to the diversity of solar cells (different absorber materials and different cell structures).

As some components of the solar module are primarily degraded by UV-range, there are some research studies on solar cell degradation under this specific range of light. Moreover, it is easier for some researching groups to study only this case because they are already equipped with a UV degradation chamber for other studies that are performing. In spite of this fact, it is important to investigate about the degradation under the full spectrum of the sunlight because solar modules installed outdoors are exposed to this spectrum.

Chapter 3: Influence of the spectrum of the light

In order to analyse the aging under different conditions, measurements of the V-I characteristics have been performed in a polycrystalline silicon solar cell with three different spectrums. In those measurements, several lights sources have been compared.

To experiment with the different spectrums two filters were created: one of them has a “UV only” transmission characteristic, so it transmits highly the range from 279 nm to 400 nm. The other filter is a “UV blocked”, and it blocks the light in the UV range (from 279 nm to 370 nm).

After the tests, the solar cell with the “UV only” filter experimented a 6,11% reduction of its maximum power, while the solar cell with the “UV blocked” filter suffered a 6,21% reduction of its maximum power. However, the solar cell exposed to the full light spectrum decreased its maximum power in a 13,35%. It is easy to verify that the degradation suffered by the full light spectrum is not due to the UV range, because the solar cells exposed to the “UV only” filter and to the “UV blocked” filter experimented almost the same decrease. The results can be seen in Fig. 3.5.

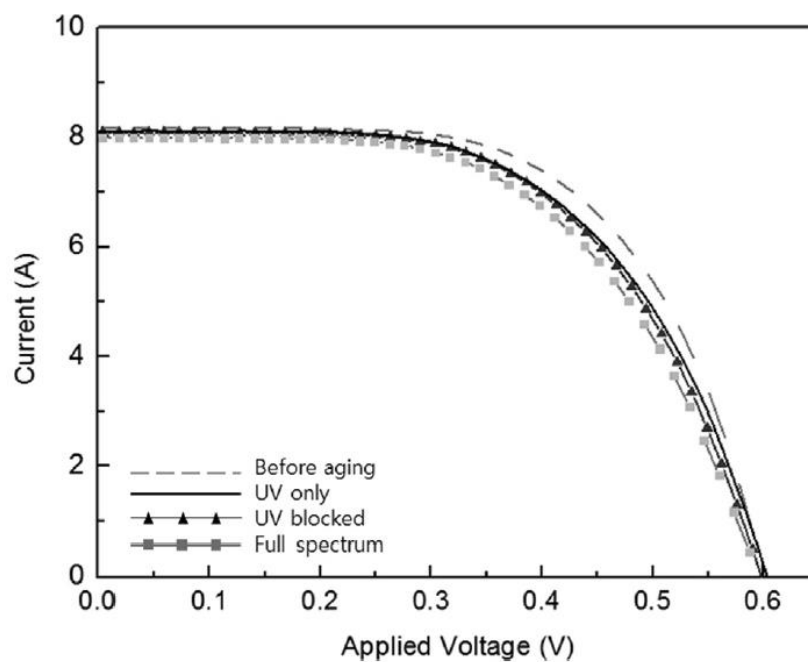


Fig. 3.5 Comparison of light soaked c-Si solar cell I-V characteristics under different filters (light intensity: 1 kW/m^2 , duration: 10h, temperature: 25°C). Source: Effectiveness of full spectrum light soaking on solar cell degradation analysis (see section 9)

4. START-UP

In this section, the designing process of the program and the circuit is explained. Moreover, the software and all the sensors used are described. Finally, the assembly of the circuit in the solar panel is explicated, and a manual for the final user is detailed

4.1. Hardware and software

In this subsection, the software and hardware used to create the application itself and the problems of the programming process are explained.

4.1.1. LabVIEW™

Several reasons led to the use of LabVIEW™ for the start-up to measure the characteristics of the solar panel. A very important motive is that LabVIEW™ is a very popular software used in the industry and in many universities with educational purposes, including the Hochschule Osnabrück. Therefore, the university already had a license and people with knowledge of the program. In addition, this software can connect with all the desired sensors, and can communicate with all the necessary protocols. Moreover, it has a visual interface that allows the user to see all the data and results graphically in a simple way; and it is rather easy to use for the final user. The program also allows sending the data to Excel® in order to analyse them later.

LabVIEW™ is the acronym of **L**aboratory **V**irtual **I**nstrumentation **E**ngineering **W**orkbench. It is a platform and a development environment to design systems, with a visual graphic programming language. It is especially recommended for creating hardware and software systems to do test, control and design (simulated or real), because it accelerates the productivity. The language that it uses is called “G language”, where G stands for graphic.

The program was created by National Instruments (NI) in 1976 to work in MAC machines. It first came out to the public in 1986, because before it was not available to purchase. Now it is available also for MAC, Windows, UNIX and Linux. The last version is 2015, which is available in demo version for students, and in professional version. The version used in this application is 2014.

The G language is a dataflow programming language. The programmer creates a structure of a graphical block diagram, wiring the blocks. The variables are propagated through these wires

Chapter 4: Start-up

and the blocks are executed as soon as their input data become available. Therefore, it is possible to execute some functions in parallel, if their input data are available at the same time. The programs created with LabVIEW™ are called VIs (Virtual Instruments), because originally they were meant to control instruments. However, nowadays it is used not only in electronic instrumentation but also in embedded programming, communications, mathematics and many others. Each VI has two different parts, the front panel and the block diagram. Sometimes there is a third part, which connects a VI with another VIs, calling them.

The front panel (Fig. 4.1) is the interface with the user. It is used to interact with the user while the program is being executed. The users can see the program's data actualized in real time. Here the controls and indicators are design. Each of these elements have a terminal assigned in the Block Diagram, and will respectively be the inputs and outputs of the program.

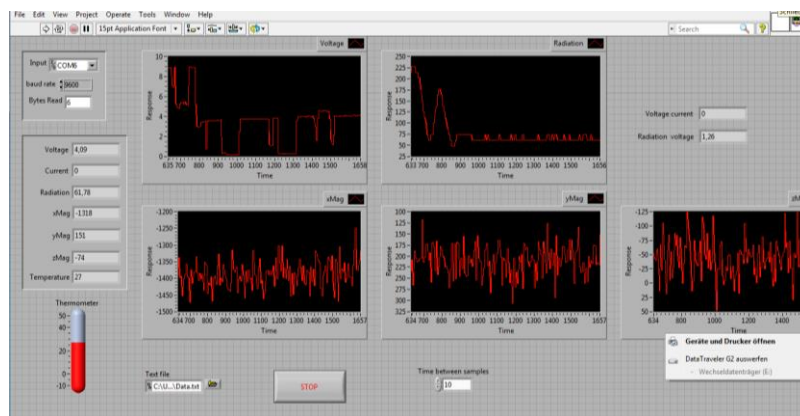


Fig. 4.1 Example of LabVIEW™ front panel

The block diagram (Fig. 4.2) is the real program, where the functions are created and interconnected. These functions perform operations on the controls and supply data to the indicators.

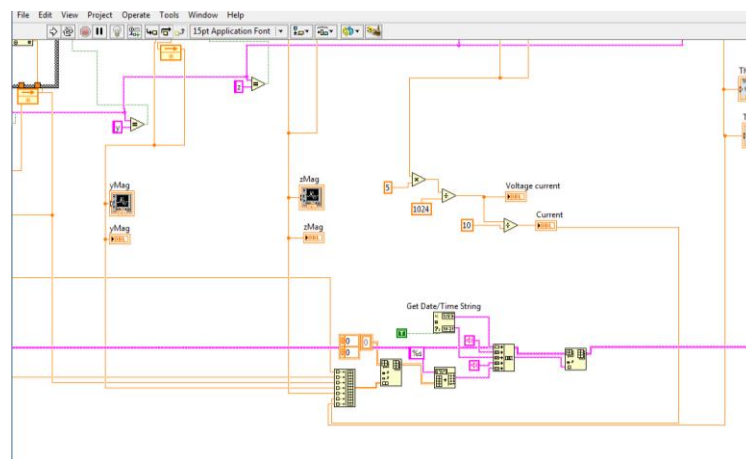


Fig. 4.2 Example of LabVIEW™ block diagram

As it has been said, it is a graphic programming tool, and that means that the programs are not written but drawn, which eases their comprehension. As there are many pre-designed blocks, it is easier for the user to create a project. Therefore, instead of taking a lot of time to program a block, this time can be invested in the graphic interface and in the interaction with the final user. It is also much easier for every kind of professionals (not only specialized programmers) to create projects because there are virtual representations of lab instruments that they already know. Besides, LabVIEW™ includes examples, documentation and tutorials in NI web page, which helps to start familiarising with this programming.

There are several advantages of using LabVIEW™ and they are the reason why it was chosen to develop the start-up of this thesis. First of all, it is possible to combine LabVIEW™ with all kind of software and hardware, both from the own manufacturer or from other companies. It is simple to communicate with other devices because it has many ways to communicate such as serial port, parallel port, USB, Bluetooth and TCP/IP communication. It can also interact with other languages or software like Matlab, CAD programs, Microsoft Office and much more.

Moreover, it has many libraries with different functions for data acquisition, signal generation, mathematics, analysis and many others. In addition, it counts with graphical interface elements to visualize the results. There are specialized libraries provided in other LabVIEW™ packages or drivers.

Furthermore, since it is an old and useful software and it has a free demo version and a cheap Student Edition, LabVIEW™ is a very popular software all over the world. That means that, as many people use it, there is a huge ecosystem (mainly in NI forums, but there are also other sites) where people share their programs; and this has helped a lot the development of the environment.

4.1.2. Software problems

However, despite the many advantages of LabVIEW™, it also presents some problems. The installation can be harsh if older versions of the program are already installed, so it is better to delete those versions first. Moreover, when using many different sensors, it is necessary to download several drivers. Some of those drivers may not be free, so the programmer should look for this information before buying the sensors. In addition, another possibility could be the use of other commands, although this could be more complicated.

Chapter 4: Start-up

Although graphic programming can be useful for simple applications, it can also be a disadvantage when coming to more complicate programs (like this case, due to all the protocol used), because it is not possible to check what happens inside the block or why there is a problem. However, with coding this is easier because the commands are written and the programmer can always see the whole program and where is the mistake.

4.1.3. NI myRIO™

At first, this device was used because it is produced by the same company as LabVIEW™, and for that reason it is easier its communication with the program. Moreover, this architecture can communicate with different protocols and sensors, which is very useful for the application since several things are being measured and therefore several sensors are used. Furthermore, NI myRIO™ has a very interesting featurig: it can communicate wireless. Therefore, it was possible to have the circuit connected to the solar panel with all the sensors in the right place; but the program could be managed from the office with a computer using only a wireless network.

NI myRIO™ is an embedded design device produced by National Instruments that is usually programmed with LabVIEW™. This company created the RIO brand, dedicated to professional engineers, to allow the creation of more complex systems. However, as its use has increased during the past years, the companies demanded more and more knowledge about RIO architecture. On account of this, NI created the NI myRIO™ device to introduce students to this architecture. With NI myRIO™, students can design real and complex engineering systems faster and with a cheaper price than with other RIO products. This device is displayed in Fig. 4.3.

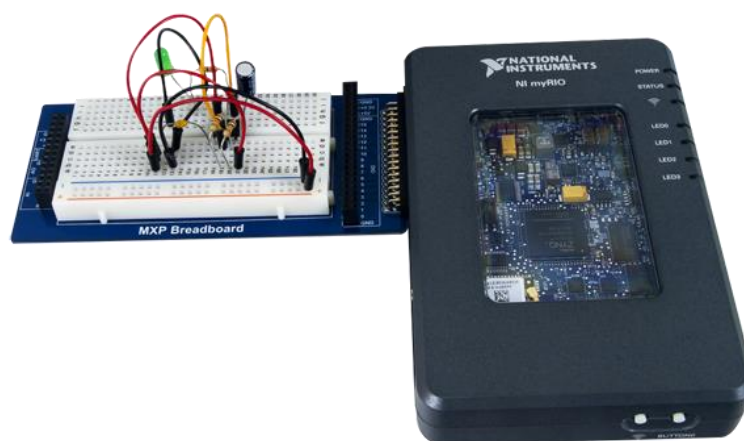


Fig. 4.3 NI myRIO

Using NI myRIO™, students can start with easy, predesigned programs and then continue creating more complex ones when they learn more about programming. In LabVIEW™ there are some blocks that are already prepared to work with NI myRIO™, what facilitates this process. In

addition, if they have already some knowledge about code programming, it is possible to program NI myRIO™ with C or C++.

This device has a Zynq chip from Xilinx, which has a FPGA and an ARM dual-core processor. The FPGA is pre-programmed to have I/O ports (input/output), so it can communicate with different protocols such as I²C, SPI and UART. Nevertheless, it is also possible to customize that afterwards if necessary.

The installation of NI myRIO™ and its drivers was not very complicated, given the examples in the NI web page and the detailed tutorial. The wireless connection with the computer was not so simple because the computer could not recognize the device. Eventually, a network called “*conectar*” was created with NI myRIO™ manager. This network is originated by the NI myRIO™ itself every time it is powered, unless the wireless function is disconnected. Then, the computer must be connected to this network (like connecting to a Wi-Fi network), and LabVIEW™ will automatically recognize the NI myRIO™ device through it. The computer will be connected to the NI myRIO™ through the Wi-Fi and to the internet through a cable, because it is impossible to connect to both networks wirelessly.

However, in the end it turned out that using so many different protocols at the same time was a bit difficult because they have different priorities and communication systems; and although it was possible to create VIs for some sensors and measure the voltage and temperature, it was very difficult to put them together in one single program afterwards. In addition, NI myRIO™ is not as old as LabVIEW™ and it is less used because it is rather specialized yet not as powerful as professional hardware like other devices of the brand RIO. That means that it was harder to find similar programs to adapt to these necessities, or to find solutions to the problems. For all these reasons in the end the application is not using NI myRIO™ anymore.

4.1.4. Arduino™

Arduino™ is a company of free hardware that produces development boards with a microcontroller and a development environment, designed to build digital devices and interactive objects in order to sense and control physical instruments. The hardware consist of an impress circuit board with a microcontroller and some analogic and digital ports of input and output, which can connect to expansion boards that amplifies the functioning characteristics of the Arduino™ board. On the other side, the software is a development environment with a programming language based on wiring.

Chapter 4: Start-up

First Arduino™ board came out in 2005, with a low price and lot of facilities to new programmers and professionals looking to design interactive projects with sensors and actuators. Since October 2012, they created new models with other types of microcontrollers. Arduino™ boards are available already assembled or in “DIY Kits” (do-it-yourself kits). The hardware designs are free available, which means anyone can build its own Arduino™ boards instead of buying one. The only limitation is that the name “Arduino” must remain only for the original products.

An Arduino™ board is composed by a microcontroller plus other components to facilitate the programming and the connection with different circuits. The boards are usually programmed via USB, although new boards are starting to incorporate other chips or methods like Bluetooth. It is also very easy to connect the Arduino™ with multiple devices thanks to its communication protocols like serial ports, I²C and SPI.

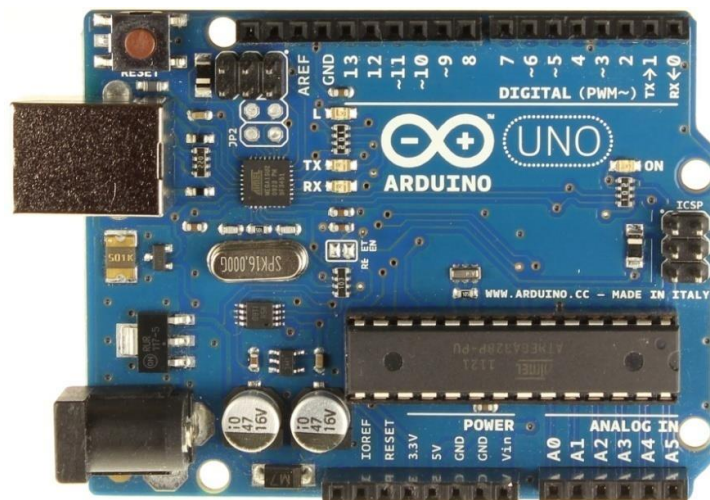


Fig. 4.4 Arduino UNO board

The programming language of Arduino™ is called Processing, and it is based on C and it has all the standard functions of C language and some of C++. The program has some examples available, which is the best way to start learning its language and to test the board. A program created in Arduino™ is called sketch and it usually has two parts. The first one is `setup()`, which is a function that runs only once at the beginning of the program to initialize the settings. The second one is `loop()`, which is a function called repeatedly until the board is disconnected or the program is closed.

The main advantage of the Arduino™ board is that the software is free and the boards are not expensive. That makes Arduino™ one of the most used programming devices in the world, both for educational purposes in universities and for individuals that want to create a project on their

own. For this reason, there is a huge community of Arduino™ users on forums, and it is easy to find programs for the applications you need or to find solutions for the problems you have.

The choice of the Arduino™ architecture was due to its low price and its free software. In addition, because it permits all the measurements with only one device. Moreover, for its simplicity and its easy programming, and finally for its community that helped to solve some problems that during the development.

Between all the different boards of Arduino™, in the beginning Arduino™ Uno (Fig. 4.4) was chosen because it has all the necessary pins and connections. It has an ATmega328P, which is enough for this application; and it can be connected to the computer via USB. This is the first model in the Arduino™ series via USB, and therefore it is the easiest to use and program and the cheapest.

However, in the end the Arduino™ Nano (Fig. 4.5) was used, mainly because of its small size. This board has also the needed specifications to accomplish the goals and it can be connected through a Mini-B USB to the computer; but its dimensions are reduced which makes easier the creation of a small device containing all the circuit. Therefore, it will be easier to move and attach to the solar panel with this reduced size.

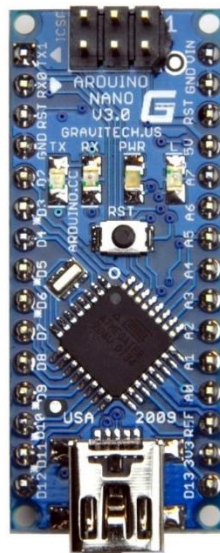


Fig. 4.5 Arduino™ Nano board

4.2. Voltage measurement

The measurement of the voltage is quite easy due to the Arduino™ having analogue ports that can receive until 5 volts. The main issue is that the solar panel has a nominal voltage of 21.5 V

Chapter 4: Start-up

and therefore it will burn the Arduino™ when directly connected. So in order to solve this problem, voltage divider was created to reduce the voltage that enters through the port; and with this new circuit it is possible to measure voltage until 51 volts. The connections can be seen in Fig. 4.6 below.

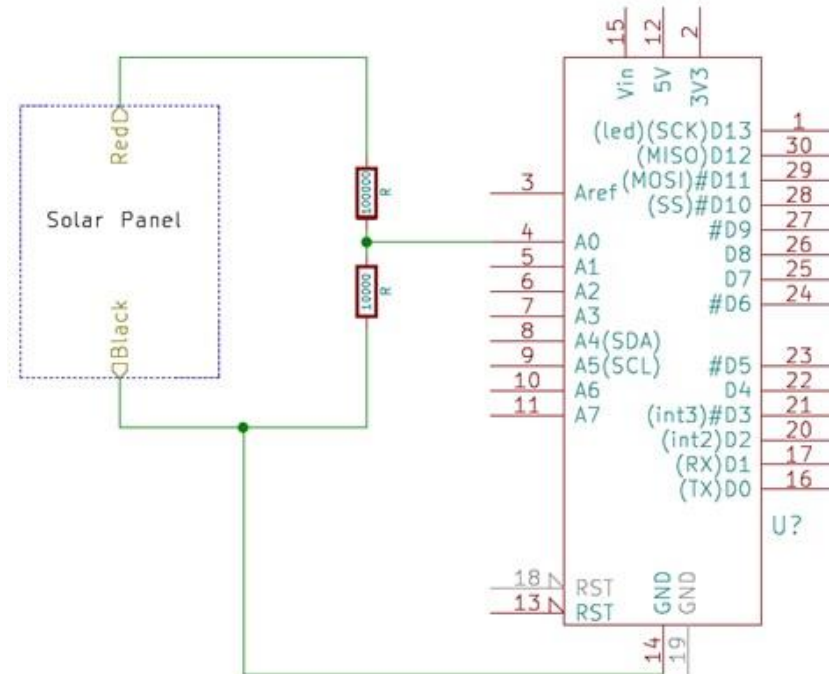


Fig. 4.6 Circuit for the voltage measurement

The solar panel has two connections and the desired measurement was the voltage difference between them. That is the reason why one is connected to the ground (black) and the other one to the input (red), because this way the voltage difference is equal to the red voltage. The formula of the voltage divider is:

$$V_{out} = \frac{R_2}{R_1 + R_2} \cdot V_{in} \quad \text{Equation 3}$$

In this case $R_1 = 100000 \Omega$ and $R_2 = 10000 \Omega$. The analogue port that is the input of the circuit is A0.

4.3. Temperature measurement

In this subsection, the process of the temperature measurement will be explained. Firstly it is necessary to clarify the utilized protocol and detail its functioning. Then the sensor and its characteristics will be described, and finally the circuit and the connections will be illustrated.

4.3.1. 1-Wire® protocol

1-Wire® is a communication protocol designed for Dallas Semiconductor. It is based on a bus, a master and several slaves and one line of data that supplies them. It also needs a common ground for all devices. The data line/supply requires a pull-up resistor connected to the supply to get the energy. This protocol is similar to I²C but it has lower data rates and longer range. It is commonly used to communicate with small cheap devices. An example of the communications between the master and the slave with this protocol is showed in Fig. 4.7.

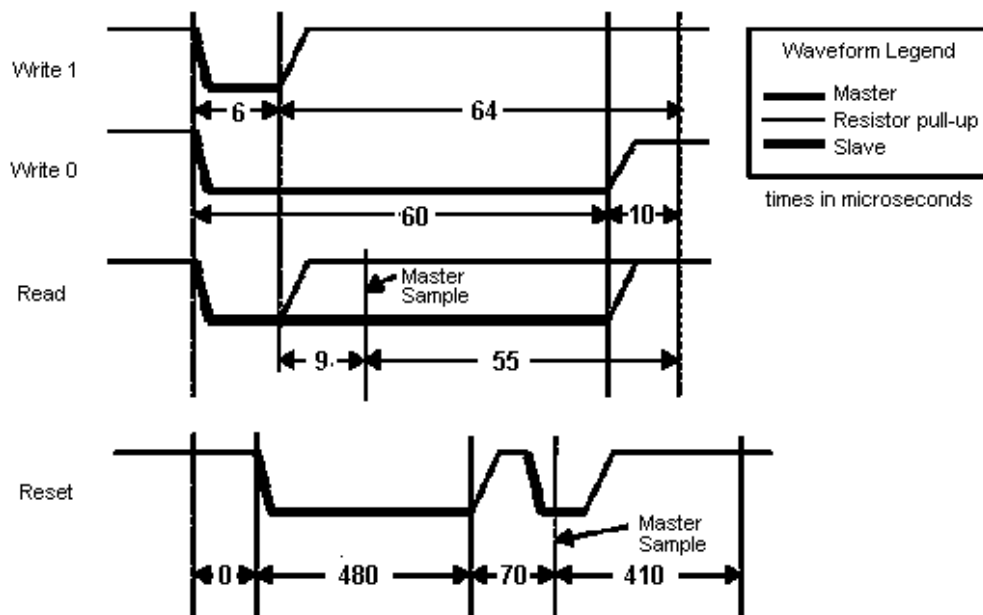


Fig. 4.7 Communication between the master and the slave in 1-Wire protocol

To begin the communication it is necessary to reset the bus. In order to do this, the master pulls the wire to 0 volts during at least 480 microseconds, and that resets all the slaves connected to the bus. Then every slave demonstrates its presence holding the bus low for at least 60 microseconds. To send a bit on 1, the master takes the data line to 0 volts during 1-15 microseconds. To send a bit on 0 it is the same but during 60 microseconds. The slave devices reads the bit approximately 30 microseconds after. The data are sent and receive in groups of 8 bits.

Since it is possible to have several devices connected, the protocol includes a unique ID of 64 bits. Of these bits the most significant byte indicates the device type and the last is an error code detector of 8 bits.

4.3.2. Sensor DS18B20

The DS18B20 sensor (Fig. 4.8) is a device that communicates digitally. It is manufactured by Maxim IC. The sensor measures automatically in degrees Celsius, which fulfil the needs of this application. It has a range between -55 to 125°C, with an accuracy of 0,5°C in the range of -10 to 85 °C. It can measure the temperature with high precision (9 to 12- bit precision selectable by the user). The precision of 9 – 10 – 11 – 12 bits corresponds with increments of 0,5 – 0,25 – 0,125 – 0,0625 °C respectively. As the default resolution is 12-bit, this was not modified to have the most precision possible. It has three terminals: two for the voltage supply and the data line. Because of its only three connections, it is ideal for multisensory systems. Each sensor has a unique 64-bit serial number, which allows the use of many sensors in one data bus because the device can address to one specific sensor using its serial number. It is also very fast since it can convert the temperature to a 12-bit digital word in a maximum of 750 ms. It uses the 1-Wire® interface, which means it needs only one port pin to communicate.

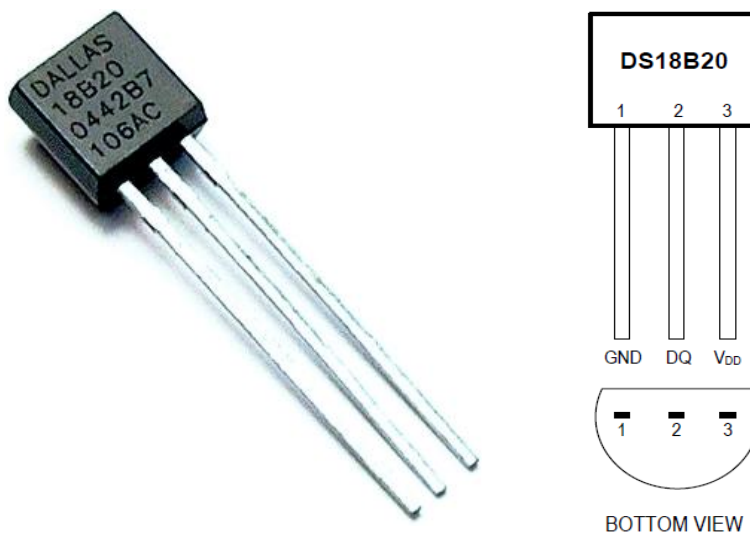


Fig. 4.8 Temperature sensor DS18B20

Another interesting characteristic of the DS18B20 is the way it is powered. This sensor can function without an external power supply. The power is supplied through the data line instead, using a pull-up resistor of approximately 5 k Ω (in this circuit it is 4k7). This way, when the bus is high, the power keeps running the sensor. It also charges an internal capacitor (CPP) that provides the energy when the bus is low and therefore not receiving energy. When using this technique, the VDD pin has to be connected to the ground. This method is called “parasite power”, and it is very useful when the space is reduced as in this case. However, it is also possible to supply energy on VDD pin like a regular sensor, which is called “external power”. This other connection is recommended when the temperatures can reach values over 100 °C.

This sensor was chosen because it is rather accurate in the required range of temperatures. Furthermore, its price is very low and it is very easy to use. The speed of conversion is fast enough, and it is a really popular sensor to measure the temperature, so it has been simple to find information about it and learn how to program the measurement.

4.3.3. Application

The measurement of the temperature has been also easy because Arduino™ can receive data with the 1-Wire® protocol. It only needs a special programming, but not a difficult connection. The pins number 1 and 3 are connected together to the ground. The middle pin transmits the data to the digital port D2 and receives also the 5 V power through a pull-up (in this case, a resistor of 4,7 kΩ). The signal is obviously digital and then the program is written to decode it. It is possible to see the circuit in Fig. 4.9 below.

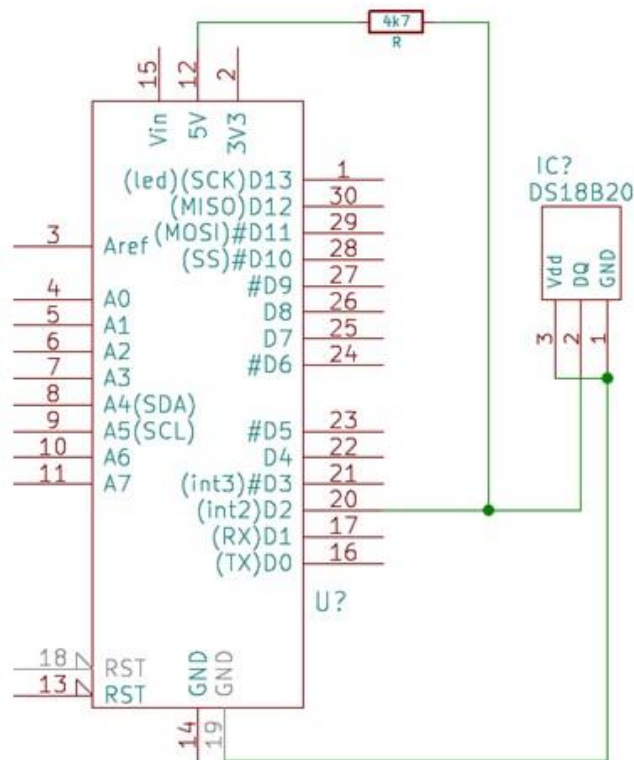


Fig. 4.9 Circuit of the temperature measurement

4.4. Angle measurement

In this subsection, the design of the circuit that measures the angle is explained. First the used protocol (in this case it is I²C protocol) will be explicated. Then the assembly of the circuit and the programming will be detailed.

4.4.1. Protocol I²C

I²C (Inter-Integrated Circuit) is a serial data bus developed in 1982 by Philips Semiconductors. It is used mainly internally for the communication between the different parts of a circuit, usually between the controller and the peripheral devices.

It is designed as a master-slave bus. The data transfer is always made by a master, the slave only reacts. It is possible to have several masters. The I²C needs two signal lines: clock (CLK) and the data line (SDA, Serial Data). Both lines need pull-up resistors to VDD.

The clock signal is always generated by the master. For each specified mode, it is predefined a maximum clock pulse allowed. It is possible to use a slower clock signal; but some devices need a minimum frequency to work correctly. Every device that can support an I²C protocol has a predetermined address, fixed by the manufacturer. The last 3 bits (subaddress) can be fixed by three control pins. This allows to have until 8 integrated device in one bus.

To begin the communication, there is an initial signal send by the master, followed by the address. This is confirmed by the acknowledgement bit of the correspondent slave. Then the master transmits a command byte, which must be acknowledged by the slave. If the master wants to read the data, it has to address the slave again plus a set bit to indicate its intentions to reading. The slave sends the Status Byte with the information, which is acknowledged by the master too. The transmission is then finished by a stop signal. It is also possible to send a reset signal to begin a new transmission, without finishing the previous one. There is an example in Fig. 4.10.

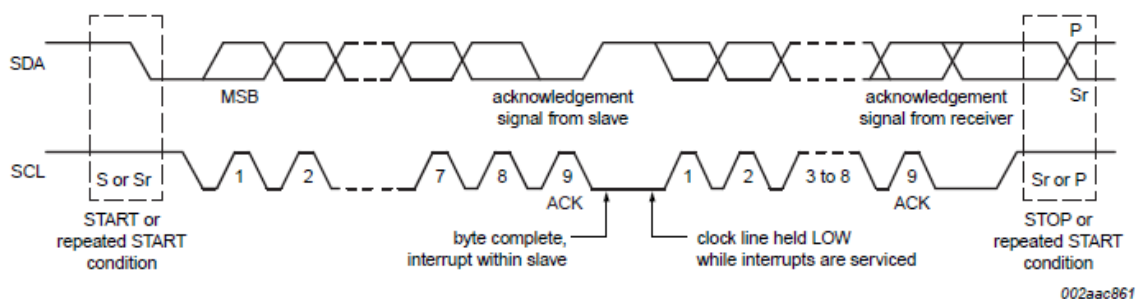


Fig. 4.10 Communication between master and slave in I²C protocol

I²C is a bit slower than the newest bus systems. However, it is very cheap because it needs few pins and that reduces the size (and therefore the cost) a lot. For this reason, it is beneficial for the peripheral systems that do not need to be fast. It is usually used for transmitting control and configuration data. Although it is a simple protocol, it is also very susceptible to interferences.

That means it should be used only in environments with few interferences, noise or compatibility problems.

This protocol was chosen because it is really simple and easy to program. It is also very popular due to its low cost, which means it is easy to find examples of its programming. Its velocity is enough for the application and this environment does not have many interferences, so it is a very appropriate protocol.

4.4.2. Magnetometer Melexis MLX90393 Triaxis® Micropower Magnetometers

The Melexis MLX90393 Triaxis® Micropower Magnetometers (Fig. 4.11) is a magnetometer produced by Melexis. Its small size allows it to fit in the smallest circuits. It senses the magnetic flux density along the three perpendicular axes of symmetry of the sensor (X, Y, Z) and then provides a digital 16-bit output proportional to that. It can also measure temperature. The raw data of the magnetic axis and the temperature is send through I²C protocol, where the magnetometer is the slave.



Fig. 4.11 Magnetometer Melexis MLX90393

The magnetometer can operate in three modes: Burst mode, Single Measurement mode and Wake-Up on Change. It is possible to change the operating mode when desired using the correct command. As the MLX90393 is only a slave, the lecture of the measured data has to be programed. It is also necessary that the master sends enough clock pulses, so it has time to read all the data bytes that it has required.

While working with I²C protocol, the MLX90393 will always acknowledge a command from the master, even if it is not a valid one. That means that after a command sent by the master the slave will always send an “acknowledgement” pulse.

Chapter 4: Start-up

As mentioned in the previous section, every device working with I²C protocol must have an address. In the case of this sensor, the address is formed by 7 bits of which the first 5 are programmed to 03 (11 in binary). The other two are defined depending on the connections of the pins A1 and A0, which by default are 0 but could be changed. This can be seen in Fig. 4.12.

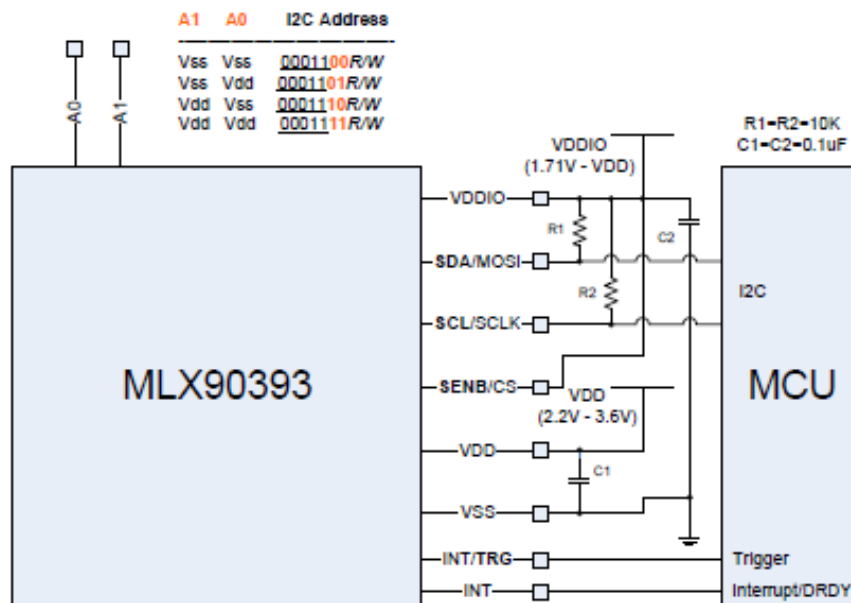


Fig. 4.12 Schematic of MLX90393 and different addresses

The chosen operation mode is the Single Measurement mode. While functioning in this mode, the master will ask for the data using the I²C protocol. With this command, the magnetometer will execute a single conversion and then return to sleep mode automatically until the next order of the master. This method consists of a single byte with the bits: z, y, x and t. The user can define with these bits which axes will be converted (or the temperature) by setting them to 1. If one of the axes or temperature is set to 0 then the sensor will not convert that magnitude (which is faster and consume less energy).

After the Single Measurement command, it is necessary to write a Read Measurement command in order to recover the data. It is also possible to select the desired data (x, y, z or t), which usually will be the same as the sensed data. The Status Byte the master will receive contains the information about the number of data bytes that are waiting to be read. If all the axes and the temperature have been required, this number will be 8. The order of the output is: T (MSB), T (LSB), X (MSB), X (LSB), Y (MSB), Y (LSB), Z (MSB), Z (LSB). If something was not asked, then that value will be skipped in the transmission.

The main advantages of this magnetometer are the size and the price. In addition, its accuracy is enough for the application and its speed is also sufficient. Furthermore, the I²C protocol is very easy to program with the Arduino™ and it functions in a stable way. Moreover, this sensor offers the possibility to measure only the outputs you are interested in, you can sense any combination of the XYZT magnitudes. Therefore, it is very easy to measure only one magnitude and it would be much faster, which allows the user to personalise the application.

Nevertheless, it is very important to be careful with this sensor. As it is rather accurate, it is also very sensitive. For this reason, it is important not to take into account every single value provided by the sensor, but to relativize all the values. That means that, if the user wants to know if there has been a movement or a rotation of the solar panel, he must not check if the values provided by the MLX90393 have changed; instead of that it is better to analyse the ensemble of the values with a graph to see the relative values of the angles.

4.4.3. Application

This circuit was a bit more difficult due to the I²C protocol. Although Arduino™ is able to transmit and receive data through this protocol; it requires a special connection plus a special programming. Besides, the sensor itself needs very specific connections to power it. The diagram can be seen in Fig. 4.13 below.

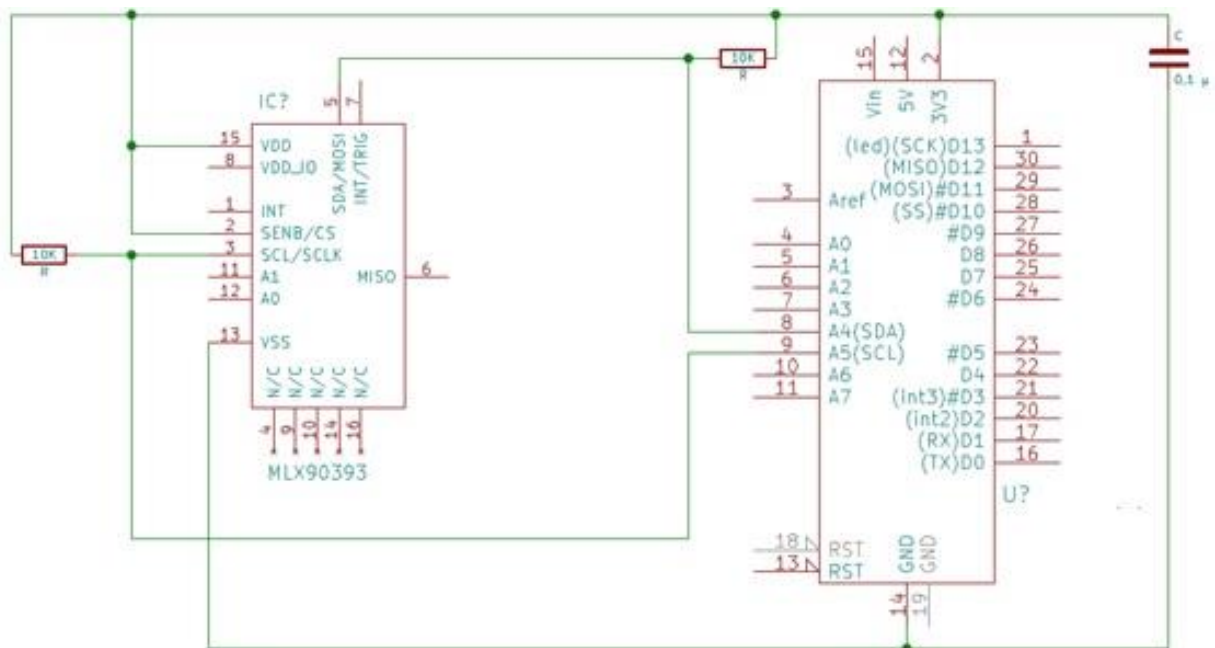


Fig. 4.13 Circuit of the angle measurement

Chapter 4: Start-up

The CS pin is connected to the 3,3 V port to pull the pin to 1. This allows the magnetometer to identify the protocol used (CS = 1 for I²C and CS = 0 for SPI). Then the VDD pin is also connected to the source of 3,3 V and the VSS pin is connected to the ground. These two pins power the sensor. For the analogue supply, the maximum limit allowed is 4 V and that is why this source was chosen instead of the 5 V one. The SDA pin (Serial Data) is the one that transmit and receive the information such as the start of the communication, the commands of read and write, and the reset. This pin is connected to the analogue port A4 because it is the hardware solution of Arduino™ for working with I²C protocol. The SCL pin is the clock, which allows the sensor and Arduino™ to synchronize when sending and receiving data. This signal is connected through analogue port A5, defined also by Arduino™. However, SDA and SCL must be connected to the 3,3 V through a pull-up too. In this case there are two resistors of 10 kΩ (one for each signal) acting as pull-up. Also, the ground and the 3,3 V source are connected with a 0,1 μF capacitor. With all the connections the magnetometer is ready to measure the angles, but it is necessary a correct programming to read the data.

4.5. Radiation measurement

In this subsection the process of the radiation measurement will be detailed. First there is an explanation about the sensor and its characteristics, and then the final circuit will be explicated and shown.

4.5.1. Sensor GBS01

The GBS01 (Fig. 4.14) is a sensor whose purpose is to measure the solar radiation (W/m²). It was developed by Technische Alternative. It has an accuracy of approximately 10% and can measure up to 1400 W/m². Its dimensions are not so big, what means it is appropriate to use in small circuits. It also has a cable of 2 m long. The communication is rather simple because the sensor creates a voltage that can be measured with a normal voltmeter, and then the conversion to global radiation is just mathematical operations.



Fig. 4.14 Radiation sensor GBS01

This sensor was chosen because of its low price. In addition, the size is perfect for attaching it to the solar panel and it has a long cable to reach the circuit even if it is placed a bit far away. Furthermore, the precision and the range are enough for this application. Moreover, the communication is very easy, so it facilitates the programming and the connections.

4.5.2. Application

As it has been said in the previous section of this document, the radiation sensor creates a voltage depending on the radiation that it perceives. Therefore, the connection is similar to the voltage measurement described in 4.2. The blue wire of the sensor is connected to the ground and the brown wire is connected to the analogue port A1 in order to transmit the voltage difference through this pin. However, in order to power the sensor to make it work, it is necessary to connect also the brown wire to a source with a pull-up. It is possible to use either 5 V or 3,3 V if the correct resistor is chosen. In this case the 5V source was chosen so the resistor must be 4,7 k Ω . The final circuit is in Fig. 4.15 below.

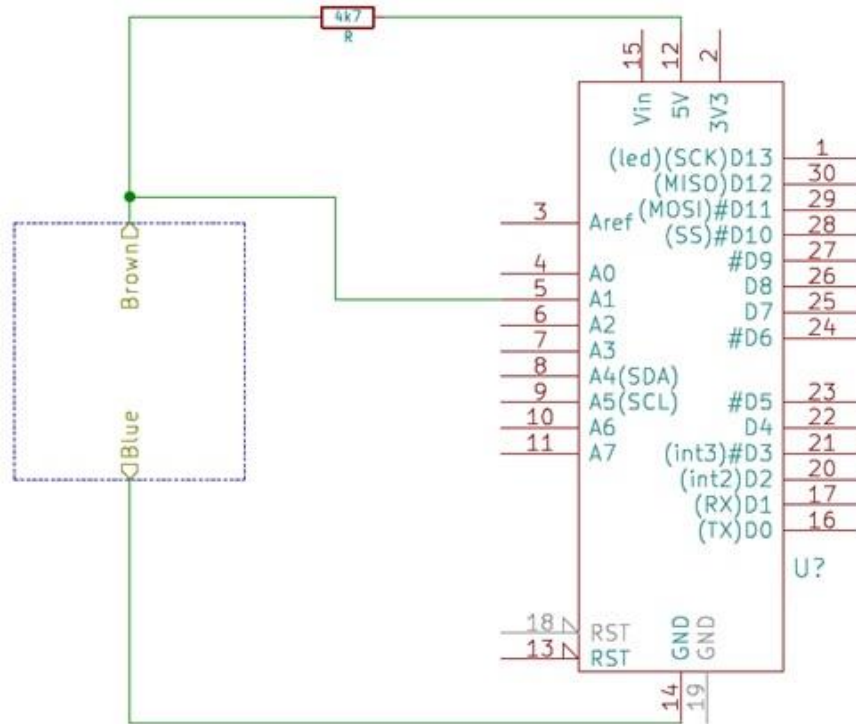


Fig. 4.15 Circuit of the radiation measurement

4.6. Current measurement

In this subsection, the process of trial and error followed to find the best solution to measure the current is detailed. Many different options have been tried and discarded, and they are explained in the next subsection. Then the characteristics of the sensor are specified; and the final circuit is explained.

4.6.1. Process

It is also interesting to measure the current provided by the solar panel, because with the voltage and the current it is possible to calculate the power generated with the formula: $P = V \cdot I$ And with the power it is possible to create the P-V curve of the solar panel and therefore characterise it.

In order to measure the current a circuit with a shunt resistor and a load was created. The load utilized is a resistor with variable value, with a maximum of 330 Ω . A shunt is a resistor used to deviate a current. Generally, the shunt value is known with a high precision and then it is useful to calculate the electric current that flows through it, as in this circuit. However, there were some problems in the designing process of this circuit.

Firstly, a resistor of 20 Ω was added. Although the circuit worked, it is impossible to measure the short-circuit current with such a high resistor. And the short-circuit current is essential to draw the characteristic P-V curve, as well as the open-circuit voltage.

For this reason, a circuit using a very small resistor like a simple wire was created. To facilitate the later transformation of voltage into current, a circuit with a drop of 1 V and a current of 1 A was made. In order to do this, an operational amplifier and four resistors (two of them of 2,2 k Ω and the others of 100 Ω) were utilized. This circuit multiplies the voltage drop 20 times, so for having 1 V in the whole circuit it is necessary to have a drop of 50 mV in the shunt resistor. Moreover, for a current of 1 A, a 50 m Ω resistor is needed, because of Ohm's law:

$$V = I \cdot R \quad \text{Equation 4}$$

As the circuit also multiplies the resistor 20 times, in the whole circuit there will be 1 Ω of resistance and therefore the current of 1 A will be maintained. Since 50 m Ω is a very small resistor, a silver wire was chosen. Metallic silver is one of the best conductors of electricity at ambient temperature with a resistivity of $1,59 \times 10^{-8} \Omega/\text{m}$ between 20 and 25°C. In order to calculate the exact 20 m Ω needed, a device based on a Wheatstone bridge that measures resistors with a very high precision was used. Specifically, a Siemens Widerstandsmessbrücke M273 A-2 that has a range between 40 m Ω and 50 k Ω . The required length to have a resistor of 50 m Ω was measured and then the circuit was completed. As the shunt resistor is only a cable and the voltage drop is very low, it can be considered like there is no resistor and therefore the measured current is the short-circuit current.

However, this circuit was not precise enough due to the resistivity of the silver changing with higher temperatures. For example, in a sunny day with 30°C the resistivity will not be the same and therefore the sensed current value is not precise.

4.6.2. Allegro™ ACS712

Finally, an ACS712 sensor (Fig. 4.16) was used to get the most precise measurement of the current. This sensor was created by Allegro™ to provide economical solutions for measuring AC or DC current in every kind of systems. It consists on a linear Hall sensor circuit with a copper conductor. When current is applied through this conductor, it generates a magnetic field that is then sensed by the Hall IC and transformed in a proportional voltage. Its accuracy is because the magnetic signal and the Hall transducer are very proximal. The resistance of the copper

Chapter 4: Start-up

conductor is $1,2 \text{ m}\Omega$ so it is a low power loss. However, it is thick enough to let the device survive at 5x overcurrent conditions. This sensor is developed in 3 different models and this can only measure up to 5 A, which is enough for the application because the short-circuit current of the solar panel is 3,73 A. Nevertheless, as the variations of the voltage is the same in every sensor, this model has the best precision.

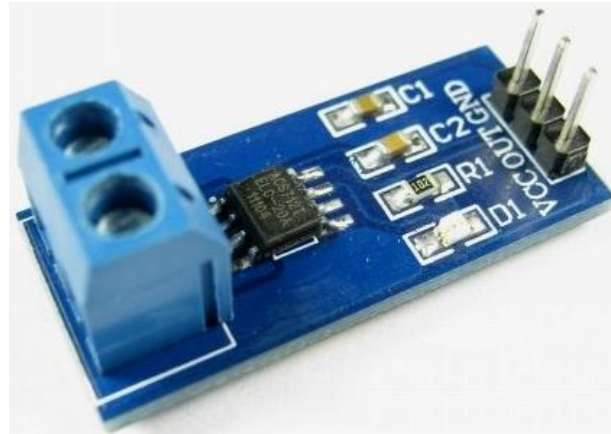


Fig. 4.16 Current sensor Allegro™ ACS712

4.6.3. Application

As the sensor generates a voltage proportional to the current that is going through it, the connection is similar to the voltage or radiation circuits. It is necessary to power the sensor with the 5 V source, and also to connect it to the ground in order to have a reference value so it is possible to measure the difference between the ground and the output pin. Analogue port A2 was chosen to connect the output voltage and receive the data.

It is also necessary to design the current circuit. The solar panel ground is connected to the ACS712, so the current is positive because it increases. Then the sensor is connected to the load, and consequently the load is connected to the red cable of the solar panel (the one with the positive voltage). The circuit can be seen in Fig. 4.17 below.

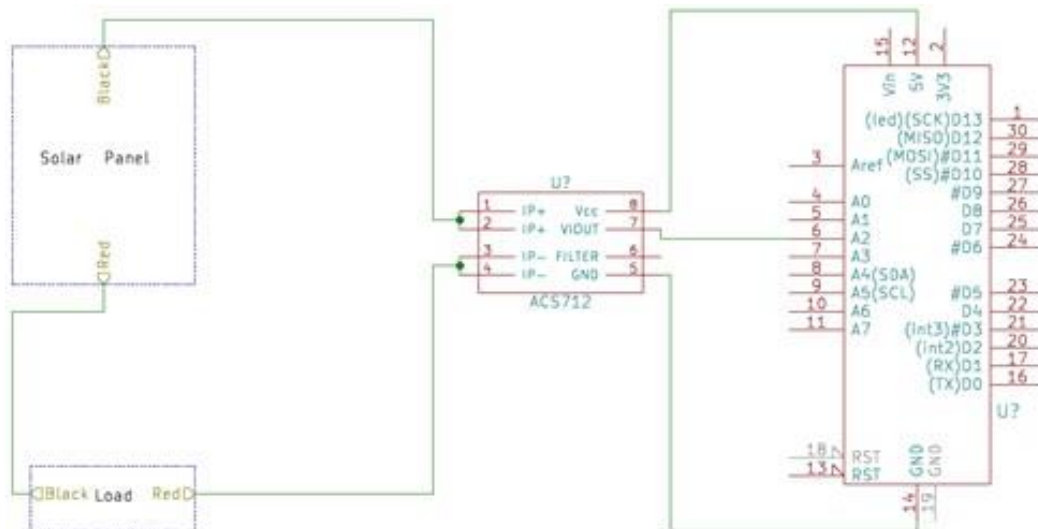


Fig. 4.17 Circuit of the current measurement

4.7. Saving data

One of the main objectives of the project was saving the data of the different measurements, in order to compare them later and extract conclusions of the impact of diverse conditions such as day, time, angle or shadows. To accomplish this goal the data of each measurement will be sent to a Microsoft Excel® file.

Microsoft Excel® (Fig. 4.18) is a calculus application distributed by Microsoft Office. Nowadays it is available for Windows, Mac, Android and iOS. It is organised in sheets, and every sheet contains a grid of cells (rows and columns). It has a complete library of statistical, engineering and financial functions. Moreover, it displays data as graphs, charts or histograms. It has also a more complex programming called macro, although this was not necessary for this application given that is only data analysis. Another advantage is that it is very easy to communicate with other Microsoft Office programs as Word, Access or Power Point in order to convert the data to another format to present them. Furthermore, it is possible to save an Excel® file with a password so the data remain safe and unmodified.

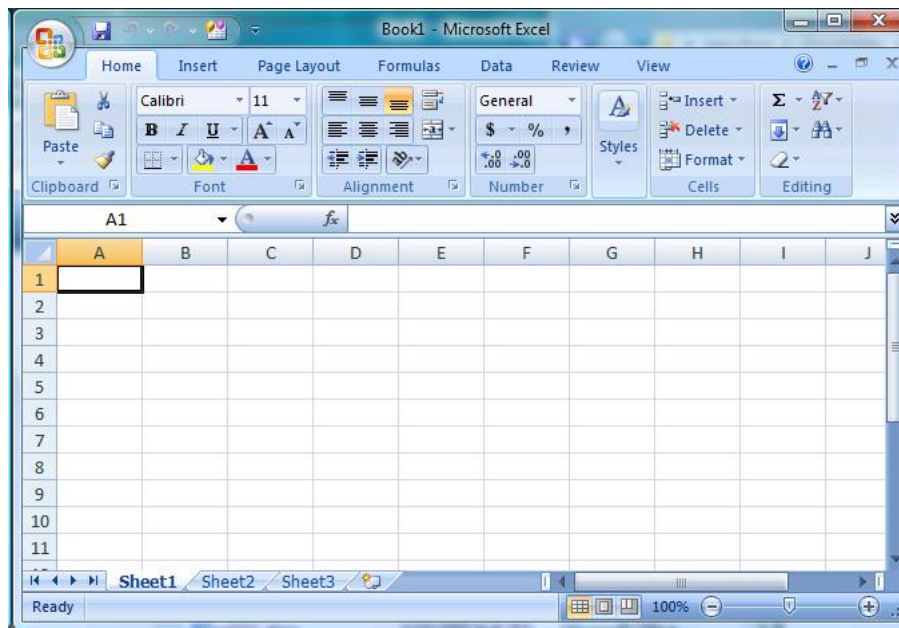


Fig. 4.18 Example of an Excel sheet

At the beginning, Microsoft Excel® was apparently the perfect program to store the data given all this advantages. It is especially interesting its plot functions, because it is very clarifying to draw the data into a graph in order to see the progressions and the changes with more perspective.

However, in order to send the data from LabVIEW™ to Microsoft Excel® it is necessary to open the Microsoft Excel® file, write the first data of the measurement (the data of the first instant) and close the Microsoft Excel® file. Then for the second sample, it has to repeat the process all over again. The problem is that Microsoft Excel® is too slow to perform all these operations fast enough, so it was only possible to take samples every 1.5 seconds and that is not sufficient for the application. Therefore, a faster program was chosen.

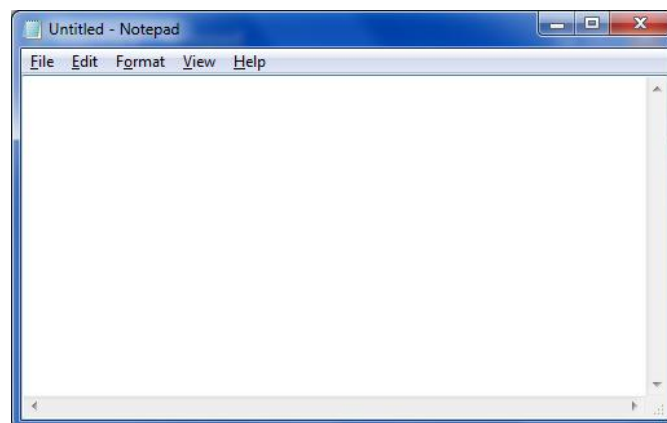


Fig. 4.19 Example of an empty Notepad file

The chosen program in the end was the Notepad (Fig. 4.19). Notepad is a simple text editor included in the Microsoft operative systems since 1985. It is a very common text-only editor. The best characteristic of the Notepad is that it can export to any text format, because its files have no format or style. As it is a very simple program, it is much faster than Microsoft Excel® and therefore is more suitable for the application. Moreover, it is possible to export the data from Notepad to Microsoft Excel® afterwards and create all the graphs or perform the required mathematical calculations.

So finally, in LabVIEW™ every sample accumulates in an array and when the measurement is complete, then the whole array is written in a text file in Notepad. A text file in a computer file that contains only text formed by normal characters without any typographic format or different fonts. Its file extension is usually txt although it is possible to have another one if the user chooses it.

4.8. Final application

In this subsection the final product will be explained. First, the Arduino™ code is written with some comments in order to detail why every command is necessary and what its functions are. Next, the LabVIEW™ program is showed in several pictures, with explanations of every block with the purpose of a better understanding of the programming. Finally, the physical circuit is explicated, as well as the assembly in the solar panel used for the experiments. A summary of all the protocols and connections can be seen in Fig. 4.20.

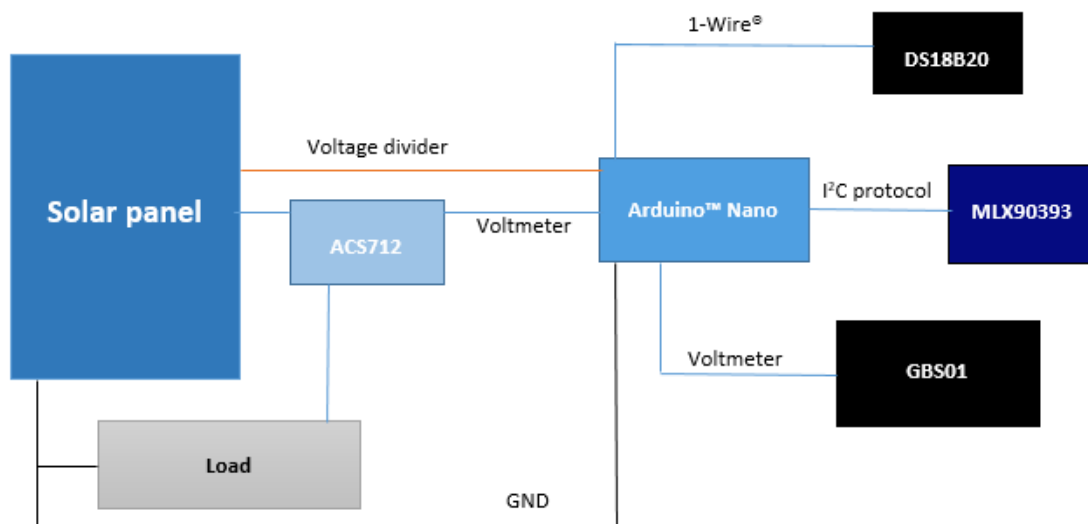


Fig. 4.20 Summary of the protocols and connections

4.8.1. In Arduino™

In this subsection, the final program created in Arduino™ and the process of the measurements will be explained. The program with the explanations is showed below.

```
#include<Wire.h> // Include the wire.h library, which is necessary to use the I2C protocol for the magnetometer.
```

```
#define Addr 0x0C // Define the address of the magnetometer as 1100 because the pins A0 and A1 are connected to 0 (by default).
```

```
#include <OneWire.h> // Include the OneWire library, which is necessary to use the 1-Wire® protocol for the temperature sensor.
```

```
#include <DallasTemperature.h> // Include the library of the Dallas company, which includes the information about this temperature sensor.
```

```
#define ONE_WIRE_BUS 2 // Define the bus used for the DS18B20. In this case digital port D2 is utilized.
```

```
OneWire oneWire(ONE_WIRE_BUS); // With this command it is possible communicate with any 1-Wire® device available.
```

```
DallasTemperature sensors(&oneWire); // Specify that the used 1-Wire® device is one of Dallas Temperature, so the program recognizes it.
```

```
void setup() { // This is the beginning of the setup section, that will initialize the program.
```

```
Wire.begin(); // The connection with the I2C protocol begins.
```

```
Serial.begin(9600); // Sets the data rate in bits per second (baud) for serial data transmission. In this case is 9600, which is the most common to communicate with the computer. The baud is a unit for symbol rate in symbols per second or pulses per second.
```

```
analogReference(DEFAULT); // Sets the analogue reference to 5 V, which is the one by default.
```

```
sensors.begin(); // This starts the library of the temperature sensor.
```

```
}
```

```
void loop() { // This is the beginning of the loop section, that will run continuously measuring until the user close the program.
```

```
    unsigned int data[7]; // The data of the bit 7 can only be a positive number from 0 to 65535 in case more space to store a data is needed.
```

```
    Wire.beginTransmission(Addr); // The master starts the transmission calling the slave with its address.
```

```
Wire.write(0x3E); // Writes the command 111110, which is the one to start the Single
Measurement Mode to read the X, Y and Z axis.
```

```
Wire.endTransmission(); // Finish the transmission with the magnetometer.
Wire.requestFrom(Addr, 1); // Ask for one byte of data to read the actual state of the
slave.
```

```
if(Wire.available() == 1) // This command is to know if the byte requested is available.
{unsigned int c = Wire.read(); // If it is available, the read it.
}
```

```
delay(100); //A delay of 100 milliseconds so the program doesn't crash for going too fast.
```

```
Wire.beginTransmission(Addr); // Another transmission starts.
```

```
Wire.write(0x4E); // Writes the command 1001110, which is the one for Read
Measurement in order to read the values of X, Y and Z axis.
```

```
Wire.endTransmission(); // Finish the transmission.
```

```
Wire.requestFrom(Addr, 7); // Ask for 7 bytes to read because it needs all the data now.
```

```
if(Wire.available() == 7); // Ask if all the bytes requested are available.
```

```
{data[0] = Wire.read(); // Read the byte 0.
```

```
data[1] = Wire.read();
```

```
data[2] = Wire.read();
```

```
data[3] = Wire.read();
```

```
data[4] = Wire.read();
```

```
data[5] = Wire.read();
```

```
data[6] = Wire.read();
```

```
}
```

```
int xValue = data[1] * 256 + data[2]; // Creates the value of the X axis by adding the byte
1 and 2 (the ones containing this information), and multiplying byte 1 per 256. This is
because it is the high byte (conformed by 8 bits) and therefore it is necessary to transform
it to the low level so the low byte can be added.
```

```
int yValue = data[3] * 256 + data[4]; // Same process to create the value of the Y axis
```

```
int zValue = data[5] * 256 + data[6];
```

```
sensors.requestTemperatures(); // Ask the DS18B20 to measure the temperature and
read it.
```

```
float T = sensors.getTempCByIndex(0); // The variable "T" is a decimal number equal to
the value read by the temperature sensor.
```

`float vValue = analogRead(0);` // The variable "vValue" is a decimal number equal to the value read in the analogue port A0, which is the voltage provided by the solar panel.

`float lecture = analogRead(1);` // The variable "lecture" is a decimal number equal to the value read in the analogue port A1, which is the voltage provided by the radiation sensor.

`float rValue = map(lecture, 0, 1023, 0, 500);` // The variable "rValue" is a decimal number equal to the voltage of the radiation sensor, but translating its scale. The scale was from 0 to 1023 bits, and now it is from 0 to 500.

`float cValue = analogRead(2);` // The variable "cValue" is a decimal number equal to the voltage read in the analogue port A2, which is the voltage measured in the shunt circuit.

`Serial.print("v");` // This command writes the letter "v" in the Monitor Serie and also in the Serial Port, to send it to LabVIEW™.

`Serial.println(vValue);` // This command does the same but writing the variable "vValue" instead, associating it with the letter "v" that is written before. It also changes the line.

`delay(200);` // There is a delay of 200 milliseconds to send the data to the Monitor Serie and to LabVIEW™.

`Serial.print("r");`

`Serial.println(rValue);`

`delay(200);`

`Serial.print("x");`

`Serial.println(xValue);`

`delay(200);`

`Serial.print("y");`

`Serial.println(yValue);`

`delay(200);`

`Serial.print("z");`

`Serial.println(zValue);`

`delay(200);`

`Serial.print("c");`

`Serial.println(cValue);`

`delay(200);`

`Serial.print("T");`

`Serial.println(T);`

`delay(200);`

}

4.8.2. In LabVIEW™

Most of the application is programmed inside a while loop, so the application will continue running until the condition of this loop is fulfilled. This way there is a continuous measurement until the user wants to finish the process. The stop condition is a big STOP button that appears in the front panel. Between every iteration of the while loop there is a pause so the program does not have problems with the conversion velocity. It is possible to choose the duration of this pause with a display in the front panel, which at the same time allows choosing the number of samples taken every second.

All the beginning part of the program is showed in Fig. 4.21. The first block is the VISA Configure Serial Port. VISA stands for Virtual Instrument Software Architecture, and it is a standard for configuring instrumentation systems such as Ethernet, USB interfaces, or Serial like in this case. Several inputs have been connected to this block, and they are explained now:

- Enable Termination Char: this is a boolean input, and if it is TRUE that means that the block will recognize the termination character.
- Termination Char: the block recognizes this character as the signal to stop reading the data from the serial port. It is by default the hexadecimal number A.
- Timeout: is the input that defines the time in milliseconds for the write and read operations. In this program is 10000, because it is the default value.
- VISA resource name: the resource that has to be opened. In the application it is the port that the user defines in the front panel (by default it is COM13).
- Baud rate: it is the rate of the transmission, settled as 9600 like the Arduino™ program.
- Data bits: number of bits in the incoming data, between 5 and 8. It is 8 by default and in this program it has not been changed.
- Parity: it is the parity used for every frame that is going to be received or emitted. It is defined as 0 by default (no parity).
- Stops bits: it is the number of stops bits that determinates the end of a frame, in this case it is 10 which indicates 1 stop bit is enough to change frames.
- Flow control: it is the type of control used by the transfer mechanism, which is none by default and in the application.

The output of this block are only two: the same VISA resource name, necessary in the next steps; and the error out, to detect if there is an error during the running of the program (for example, not detecting any serial port).

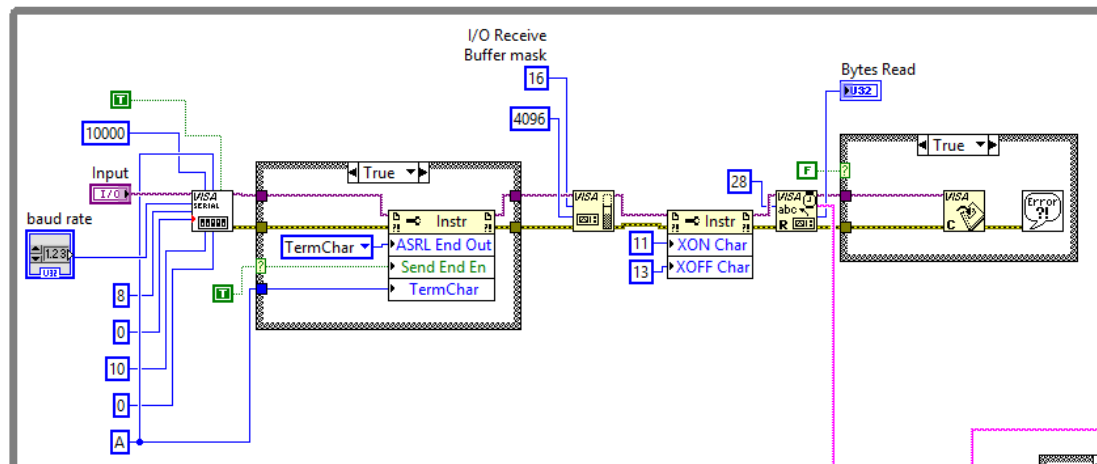


Fig. 4.21 Part 1 of the LabVIEW™ program (settings of the serial port)

The next step in the application is a case structure. This case structure contains two cases, one executes when the boolean input is TRUE and another one when the boolean input is FALSE. The FALSE case, however, is almost empty: it contains only the VISA resource name and the signal “error out” going through the case structure. Nevertheless, this case will never execute because the boolean input is a constant settled as true.

The TRUE case contains a Property Node, which is a block to read and/or write properties of a reference. LabVIEW™ has preconfigured property nodes for VISA properties. This concrete node sets 3 properties. The first one is the End Mode for Writes, which defines the method to finish write operations. TermChar (termination character) has been chosen because it is the same as for reading operations, which means that if the termination character is read all the operations will end. The second one is the Send End Enable, which is permanently settled as TRUE. This means the application will send an END signal at the end of every write operation. The third one specifies the termination character, which will be the same as the VISA input.

The subsequent block is the VISA Set I/O Buffer Size, which selects the size of the input/output buffer. This block is left with all the settings by default. Another Property Node sets the XON/XOFF to control the data flow. Both values are set by default to 11 and 13 respectively. The XOFF character is sent when the receive buffer is nearly full, so the transmission is interrupted when this character is received. The XON character is sent to enable the communication again. The upcoming block is the VISA Read, whose input is the number of bits that the user needs to read, and whose output is a string with the data received from the buffer. It has another output that shows the number of bytes that have been read in a display in the front panel.

Ensuing this block there is another case structure. The boolean input is settled as FALSE and the FALSE case is empty, which means that if everything works okay nothing will happen. The TRUE case contains a VISA Close block that closes the communication, because it is necessary to have a close block at the end of the VISA resource name wire (the communication needs an ending). There is also a Simple Error Handler so if an error happens it will provide the error code in order to identify the problem.

After that, the program separates the data in each measured property. This process can be seen in Fig. 4.22. In the Arduino™ program a letter followed by the sensed data is printed, which a string formed by one letter and some numbers is being sent to LabVIEW™. So this letter will be detected and removed from the string to obtain the final results.

Firstly, there is a block called Replace Substring, which deletes the substring at the specified offset. The inputs of this block are the mentioned offset (in this case is 0, the first position of the string), and the length of the substring that will be deleted (1, because there is only one letter to eliminate). This implies that only the first letter of the received string is deleted. The outputs are the final string (the sensed properties) and the deleted substring (the letter).

From now on, all the properties have the same structure to be read, but the voltage will be explained with more details. There is a comparison (with an equal symbol) between the deleted letter and the “v”, which is the letter that identifies the voltage (the letter serial printed with the voltage). Following to this comparison there is another case structure, and the boolean input is the result of the comparison. If the deleted letter is not equal to “v”, then the case is FALSE and it is empty, so the program will not perform any action. If the deleted letter is equal to “v” the case is TRUE. The string with the data has to be converted into a numeric format so mathematical operations with the results can be performed.

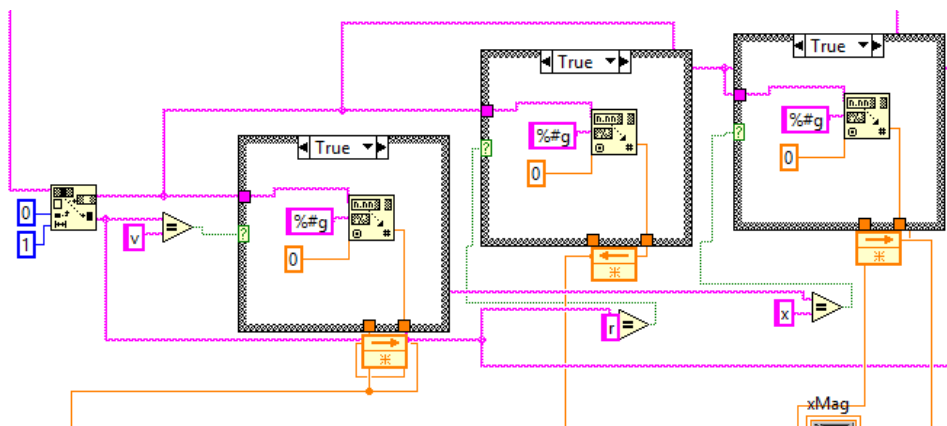


Fig. 4.22 Part 2 of the LabVIEW™ program (separation of the variables)

Chapter 4: Start-up

In order to do this there is a Scan Value block. It converts the string into a DBL format, which is a double-precision, floating-point numeric format. The format defined is `%#g`, which means that the program will choose between scientific notation (if the exponent is less than -4 or greater than the precision specified), or floating-point notation (if the exponent is greater than -4 or less than the precision specified). Subsequently there is a feedback node that stores the data between two iterations of the loop, in case one iteration fails it will keep the value from the previous one. After that, the raw data are transformed into the desired characteristics.

In the case of the voltage (Fig. 4.23), it is necessary to transform the raw data from the 0-5 V scale to the 0-1024 bits scale. In order to do this the value is multiplied by 4,7 (because it is the real output value of the Arduino, it is not 5 V) and then divide by 1024. Then the operation previously mentioned in the 4.2. subsection has to be performed, to transform the sensed value to the real value thanks to the voltage divider. Later the final voltage value is displayed in both a numeric and graphic way.

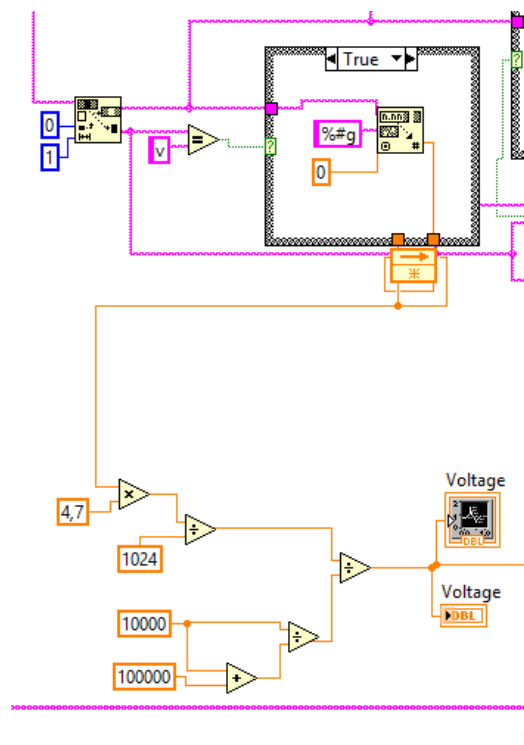


Fig. 4.23 Part 3 of the LabVIEW™ program (conversion of the voltage)

In the case of the radiation (Fig. 4.24), the scale is between 0 and 500 so the value has to be divided by 100 to obtain a scale between 0 and 5 V, which is the scale of the voltage of Arduino. After that, a rule of three is performed to get the correct radiation value. The voltage output depending of the radiation detected is showed in Fig. 4.25. The reference values chosen are 1,29 V equal 100 W/m^2 .

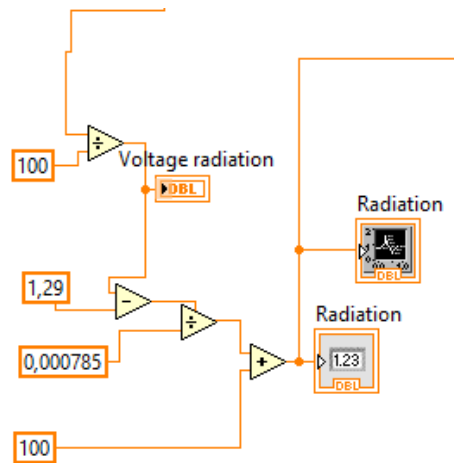


Fig. 4.24 Part 3 of the LabVIEW™ program (conversion of the radiation)

Global radiation [W/m ²]	Sensor output voltage [V]
0	1,211
100	1,290
200	1,368
300	1,447
400	1,525
500	1,604
600	1,682
700	1,761
800	1,840
900	1,918
1000	1,997
1100	2,075
1200	2,154
1300	2,233

Fig. 4.25 Relation between the radiation and the output value of the sensor BGS01

The rest of the processes are shown in Fig. 4.26. The x, y and z angles are already get in its final values so they do not need any transformation. There are showed in the front panel in a numeric display and also in a graph. The same situation is for the temperature, which is sensed in Celsius degrees and displayed in a thermometer and a numerical field.

The process to transform the current is similar to the voltage or radiation, given that the three sensors provide a voltage. First, the scale is changed from 0-4,7 V to 0-1024 bits. Then the result is divided by 0,185 because this is the sensitivity of the sensor. Then the offset, which is half of VDD, is subtracted. In this case VDD=4,7 V so the offset is 2,35 V, but dividing by 0,185 so 12,7027 A are subtracted.

Chapter 4: Start-up

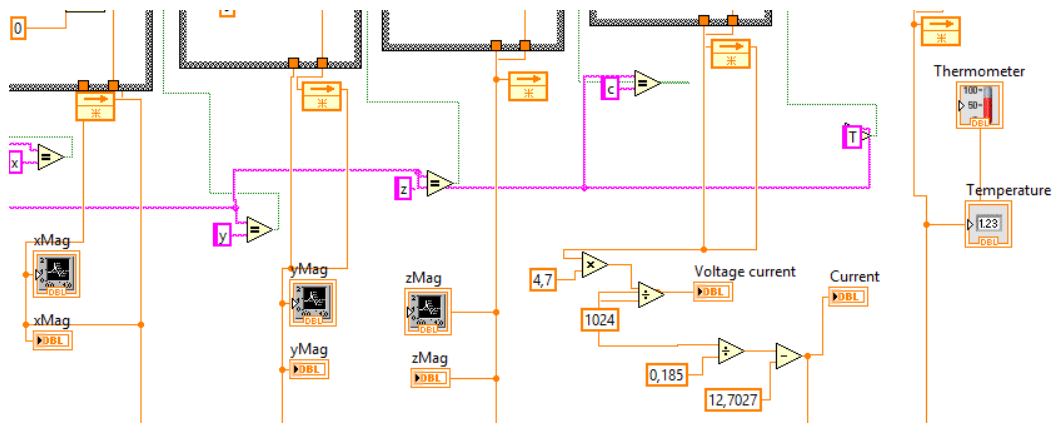


Fig. 4.26 Part 5 of the LabVIEW™ program (conversion of angles, current and temperature)

For the sending to a txt file, the essential thing is converting all the values into an array that can be easily sent. This appears in Fig. 4.27. In order to do this Build Array block is used, because it puts all the characteristics together and creates a single array. Upcoming this block there is an Insert into Array, where another array of two dimensions filled with 0 is inserted, in order to create an array of two dimensions (rows and columns). Then there is an Array to Spreadsheet String in order to convert the numeric values into text to make it possible to write them, with the format of a text string. This string is the input of the block Concatenate Strings that unites several strings. This block unifies the date, a tabulation, the time, another tabulation, and finally the string with the data. To get the date and time in real time a Get Date/Time String with seconds is used.

The concatenated string is then inserted into another Insert into Array block, that combines it with a string of one dimension that contains all the headers of the rows (Date, Time, Voltage, Radiation, X axis, Y axis, Z axis, Current, Temperature). This string is located outside of the while loop because it does not change every iteration, and it enters through a shift register. The merged new string goes out of the while loop through a shift register. The shift register saves all the strings from every iteration, and then when the while loop finishes it sends everything out to the next block.

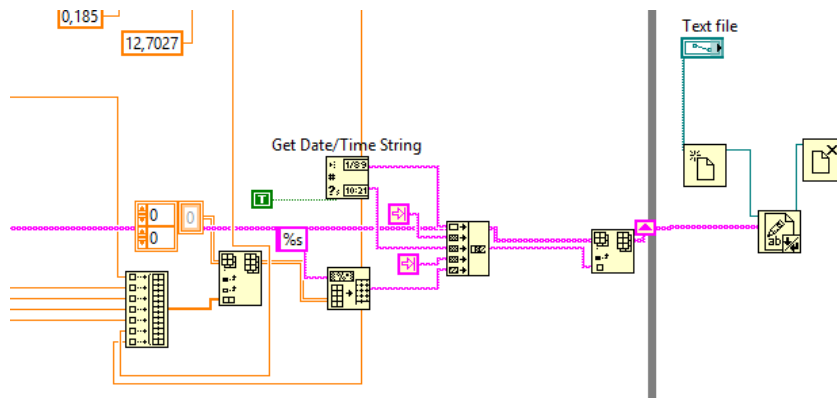


Fig. 4.27 Part 6 of the LabVIEW™ program (saving the data into a TXT file)

Following to this, and now outside the while loop, there is a Write to Text File block. The input is the string of the shift register plus a block to Open/Create/Replace File. The output is a Close File block, to finishes with the writing process. In order to select the txt file where the data will be saved, there is a display in the front panel where the user can browse and select the desired file. This display is a file path in the block diagram and it is an input of the Open/Create/Replace File block.

4.8.3. Physical circuit

After all the different circuits were created and tested, the final circuit was created by unifying all of them. Firstly, a protoboard was used to check the complete program in Arduino™ and LabVIEW™. However, the circuit could not remain in the protoboard because it was too fragile and even the slightest movement could disconnect a cable or sensor. Especially, the DS18B20 is very sensitive and it got disconnected every time. For this reason all the components were welded into a circuit board (Fig. 4.28).

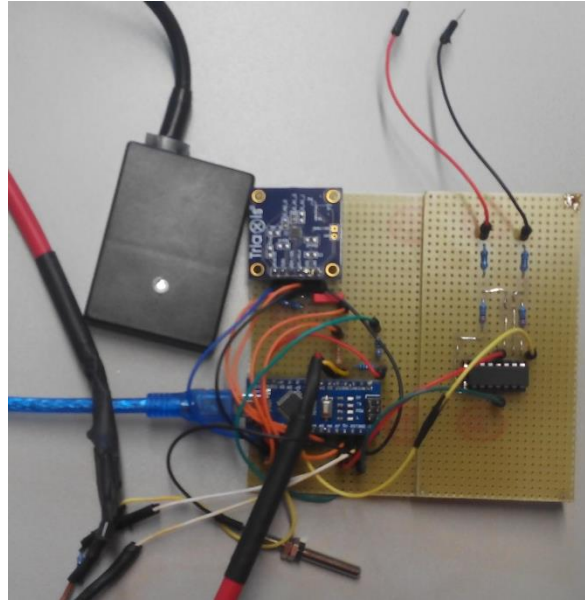


Fig. 4.28 Circuit welded (version with silver wire as shunt resistor)

Nevertheless, the temperature sensor needs to be attached to the back of the solar panel in order to measure its temperature correctly. That is why it to a long cable with three wires was welded. After that, the sensor was glued to the solar panel with a hot glue gun. Afterward, the whole circuit was attached to the panel to allow the MLX90393 to measure its angle. For this purpose several holes were drilled in the electric box of the panel, which contains the 3 cables that provide the power (one for each side of the panel and another one for the middle). The circuit was attached to this box using one bridle to fix it there, but at the same time it is a very flexible system that permits the dismantling of the circuit if necessary.

Finally, as the cable of the Arduino™ Nano is very short, an USB extensor of 2 metres was used to have enough length to connect all the system to the computer in order to upload the Arduino™ program to the board and receive the data in Arduino™ and LabVIEW™ after that. The problem is that when the solar panel was moved, the cables were all the time floating in the air and therefore by the effect of gravity, the Arduino™ cable and the USB extensor disconnected quite often. That interrupts the communication and it is necessary to restart the measurement again, it is not possible to reconnect them and continue with the process. Consequently, both cables were joined with a piece of rigid plastic and two bridles and now they are stick together and cannot be disconnected. The final result is shown in Fig. 4.29.

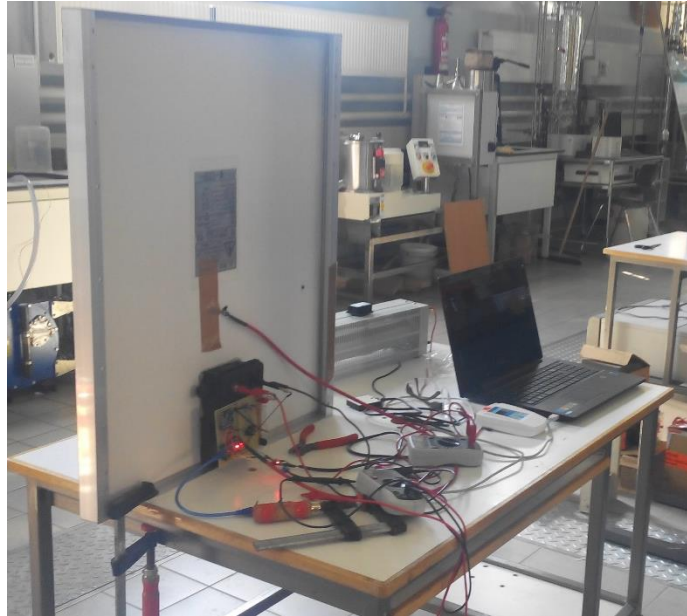


Fig. 4.29 Final assembly

4.9. Manual of the program for the final user

The program is visual, intuitive and simple. It automatically measures all the magnitudes of interest and provides the results in a numeric and graphic environment. In order to setup the program, it is first necessary to select the desired time between samples. This time is defined in milliseconds. It means that, if the user select 10 milliseconds between samples, the program will perform 100 measurements in 1 second. For this operation the user has to click in the white rectangle and write the number (Fig. 4.30).

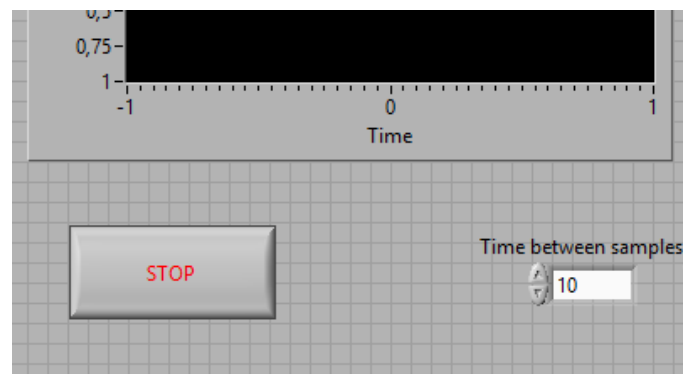


Fig. 4.30 Display with the time between samples (modifiable by the user)

Afterwards the user has to specify in which txt file does he wants to save the data. It is possible to choose an existent file or to create one in this moment. To indicate this file, the user has to click in the folder (Fig. 4.31). Then he has to explore in the computer folders until he finds the desired file, or create a new one (by right clicking and selecting New – Text document).



Fig. 4.31 Display to select the TXT file where the data will be saved

The next step is selecting the correct input port where Arduino™ (and the whole circuit) is connected. The user must click in the arrow next to the port selected (by default it is COM13) and choose the port that appears right under, usually COM4, COM6 or COM8. This can be seen in Fig. 4.32.

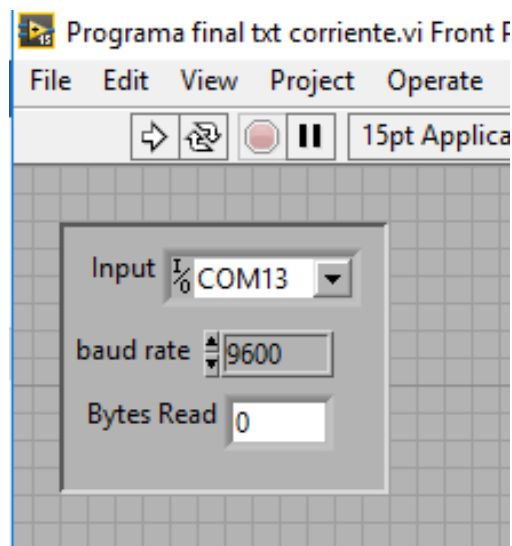


Fig. 4.32 Display where the user must select the Arduino™ port

After these 3 operations, the program is ready to function. In order to start measuring, the user has to click the run white single arrow in the top of the panel, under the menus. It is important not to click the two arrows in the shape of a circle, because this button is to run the program continuously and this program is already a continuous while loop, so it would be a loop inside a cycle and that can result in obstructions and problems.

Once the program is running, the output values appear in numeric displays on the left side of the panel (Fig. 4.33). Those are the most important outputs, the ones required in the objectives of the thesis. However, on the right side it is possible to see also the voltage generated by the ACS712 (voltage current) and by the GSB01 (radiation current), so these values are visible to check in case the results are not logical. This appears in Fig. 4.34. In the graphs the voltage, the radiation, and the 3 sensed angles are displayed. On the left bottom corner of the panel there is a thermometer that shows the temperature sensed by the DS18B20.

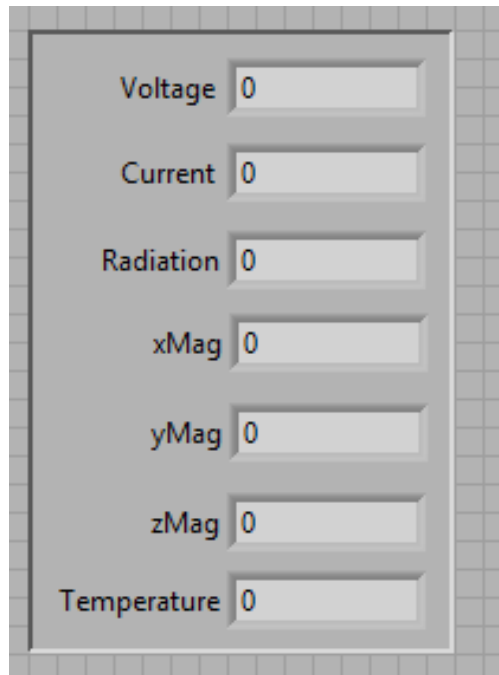


Fig. 4.33 Displays with the results of the measurements (left side of the front panel)

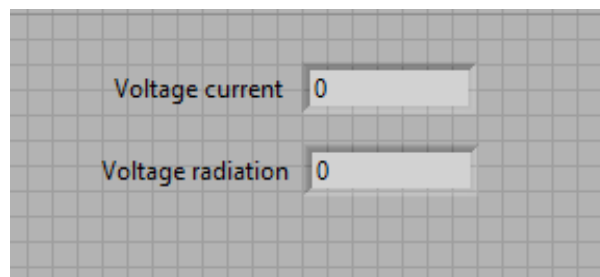


Fig. 4.34 Displays with variables to check the correct performance of the program (right side of the front panel)

During the measurement process, it is possible to change the value of the variable resistor by moving the black piece located on top of it. By doing this the user will receive different outputs and therefore it is possible to draw the characteristic P-V curve with those different values.

When the user has all the required results and he would like to stop the measurement, he only needs to press the STOP button (Fig. 4.35) placed on the bottom of the panel. It is fundamental to press this button, and not the red button set next to the arrows under the menus on the top. That is because the STOP button just finishes the while loop, and then the program writes all the collected data into the selected txt file and stops running (because it has already ended). Nevertheless, the red button on the top finishes the program in the very moment it is pressed, without letting it write in the txt file, so the data are not saved if the program is stopped this way.



Fig. 4.35 Stop button (bottom of the front panel).

Thereafter the user has all the data saved in the txt file to use them when it is necessary. It is also possible to export this data into an Excel® file to create graphs, charts, or perform mathematical operations with them. In order to do this the user should open Microsoft Excel®, the click “Open”, select “All files” and choose the txt file with the data. By running the program several times under different conditions, it is possible to learn about the effect of the environment in the generation of solar photovoltaic energy.

It is important to be careful when repeating a measurement. If the user wants to repeat a measurement and rewrite the results, he must first delete the content of the text file. If he does not clean the file, then the new results will be overwritten over the old results, and if the measurement last shorter than the previous one then he will have a mix of data. The first data will be the new ones, and then below he will have part of the old data. This can lead to confusion, which is why it is essential to clean the files or create a new file to save the new data.

5. RESULTS

In this section the results obtained in several measurements under different conditions will be explained. In every measurement different characteristics were taken into account so diverse magnitudes will be highlighted in each one.

5.1. Measurement 1

The first measurement was taken indoors with small halogen lights, and using only the one located on top of them. The lamp is one metre away from the panel and the panel is vertical over the table. The load is settled in the middle and, as a shunt, a resistor of 10Ω is used, which is not the final circuit for measuring the current but this is not important yet.

The first results should not be taken into account because the application is still starting and therefore in its transitory period. For this reason, the results are not valid. After the first measurements, the voltage becomes pretty stable because the light source is approximately constant, with the same intensity, and located in the exact same place.

The radiation values increase in the beginning until they reach a maximum value of $138,22 \text{ W/m}^2$ and then decrease again. This is due to the alternating current that powers the lamps, so the radiation differs depending on the cycle of the current. This can be seen because the rising values are the same as the falling values; so it is a symmetric cycle.

The temperature oscillates between 24 and 25°C , although it tends to be higher at the end of the measuring because the panel gets hotter when producing energy. The angles remain stable because the panel is vertically fixed to the table.

5.2. Measurement 2

The conditions of this measurement are similar to the Measurement 1, but using 2 halogen lamps this time (the top one and the middle one). However, this does not affect the power production as perceived in the voltage. Nevertheless, it does affect the radiation because it is much higher than in the previous measurement; and the temperature has augmented a lot due to the heating effect of this kind of lamps.

5.3. Measurement 3

This time the three lamps are being used to measure the characteristics. The voltage is higher and the radiation is greater too, comparing with the previous measurement. The temperature is not as high because this test was made before the Measurement 2, and therefore the panel was not so hot yet. However, it is possible to see the evolution of the temperature starting with Measurement 1.

5.4. Measurement 4

In this occasion the conditions are the same as in Measurement 3 but the lamps are located 0,5 metres away from the solar panel. It is easy to check that the voltage and radiation are bigger than in the previous subsection. Moreover, the temperature increases much faster than in previous measurements due to the heating effect of the lamps, which is much greater now because of the short distance. The voltage values are similar to a measurement outside with natural sun. This means, to obtain the same power as a sunny day in Germany, it is necessary to use three halogen lamps very near to the solar panel because the artificial light is not as good to generate solar power.

5.5. Measurement 5

In this event the conditions remain the same as in the measurement 3, but the load changes its value. The selector of the load was moved all the way to the right and then all the way to the left, therefore changing the resistor and the power. It is possible to see that the voltage increases and then decreases again for this reason. However, the radiation is stable, so in this case it is not due to the alternating current cycle but because of the changes of the load.

5.6. Measurement 6

This measurement was made indoors and without halogen lamps, because it was only to check the performance of the MLX90393. The panel was placed vertically on the table and then it made a 90° rotation around the X-axis. This means that the panel remains vertical on the table but is facing to another wall. Then the panel was put in the initial position again. The rotation is manual so it is not very precise, although when using the solar panel with PV tracker the movement will be more precise. The temperature sensor broke due to the movement so the values of the temperature are not valid.

In order to appreciate the results better, the data have been sent from the txt file to an Microsoft Excel® file. Then with the angles values a graphic has been created in order to analyse the results with a better perspective. As seen in the graphic below (Fig. 5.1), the results are not very good because the rotation cannot be perceived. This is because the movement is not precise and because when rotating there are also movements in other axis. Furthermore, the rotation is not exactly around the X-axis of the sensor, it is around one edge of the panel, so the sensor does not remain in the same place and therefore it is more difficult to see the results.

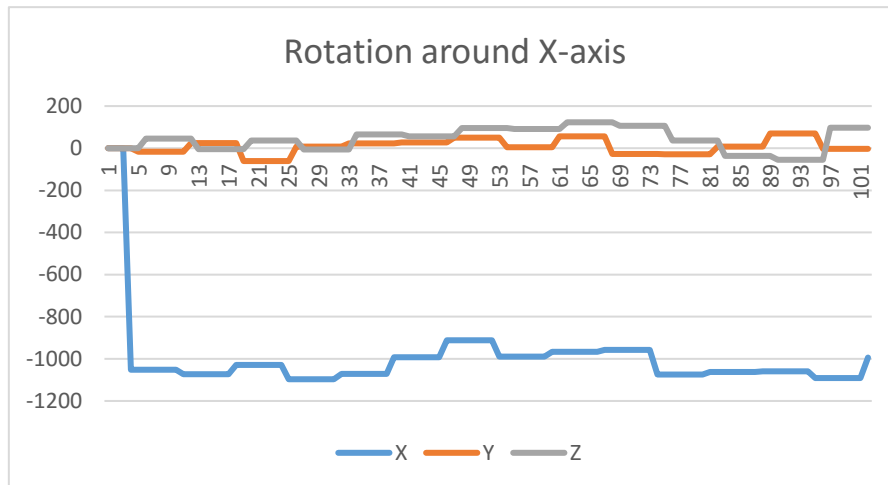


Fig. 5.1 Graphic created in Microsoft Excel® showing the results of Measurement 6

5.7. Measurement 7

This case is similar to the previous subsection, but now the rotation happens around the Y-axis. This means that the panel starts vertical on the table, then it is placed horizontal with the front side against the table, and then it recovers the initial position. The rest of the conditions are the same.

Now it is possible to see in the graphic below (Fig. 5.2) that this time the rotation is more evident, at least in the X-axis. The values of this axis start stable, then there is a brusque change, they are steady in the new position too, and then another abrupt modification to recover the original values.

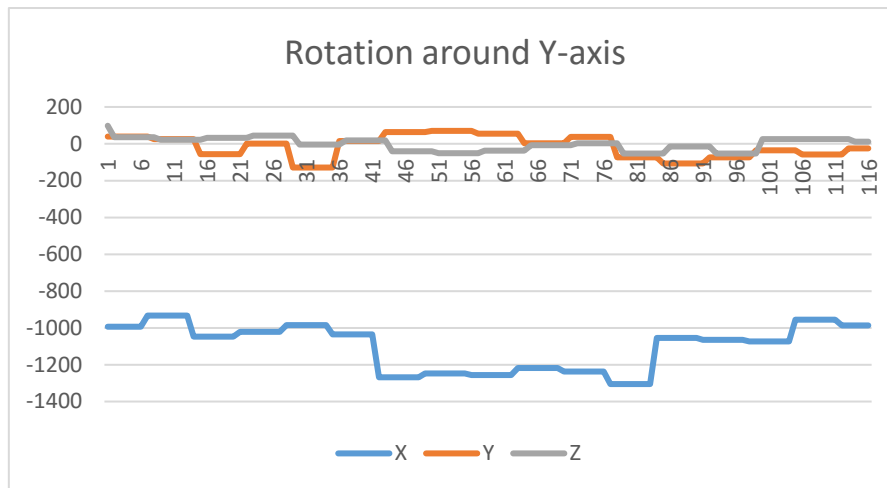


Fig. 5.2 Graphic created in Microsoft Excel® showing the results of Measurement 7

5.8. Measurement 8

Finally the measurement was repeated but rotating around the Z-axis, which signifies that the solar panel faces all the time the same wall but at first it is vertical on one of its short sides, and then it lays on one of its long sides. The rest of the experiment is performed under the same conditions.

In this occasion it is easier to check the rotation in Fig. 5.3. The values of the Z-axis are approximately constant, while the values of the X-axis and Y-axis have a sudden change at the same moment due to the rotation and then the original values are restored.

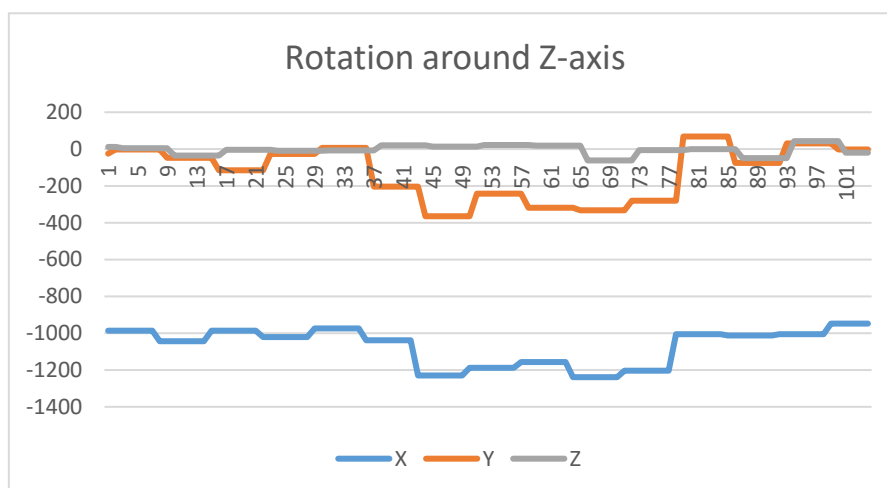


Fig. 5.3 Graphic created in Microsoft Excel® showing the results of Measurement 8

5.9. Measurement 9

Now a measurement with all the rotations was performed. The panel started vertical on one of its shorter sides and then the different rotations happened successively, but after every rotation the original position is recovered. The results can be seen in Fig. 5.4.

Although the values of the Z-axis seem constant, the changes can be appreciated in the other axis. At first the X-axis is stable, while a small alteration in the Y-axis. Then the Y-axis continue steady while there is a huge variation in the X-axis. Finally the simultaneous modification of the X- and Y-axis can be seen while the rotation of the Z-axis takes place.

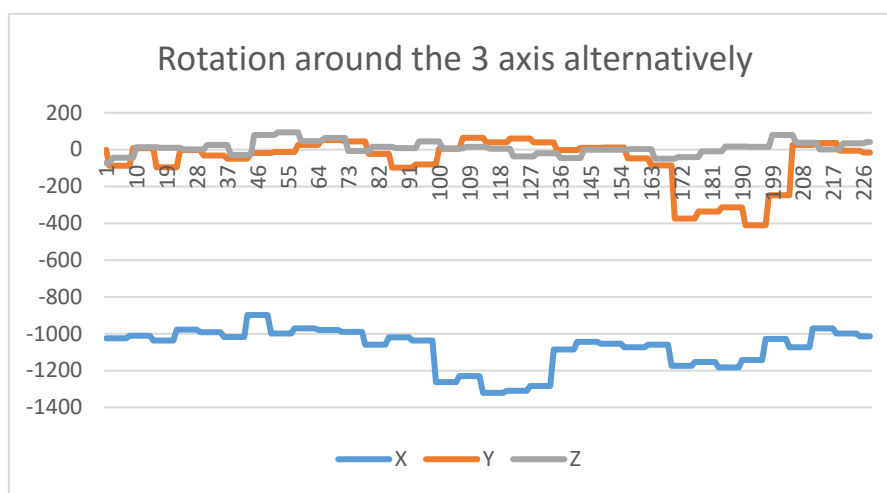


Fig. 5.4 Graphic created in Microsoft Excel® showing the results of Measurement 9

5.10. Measurement 10

This experiment was executed outside the 20th June, at 11:30 in the morning. The final circuit for the current was not created yet so it is only a checking of the other sensors. As seen in the data, the radiation is rather high. It increases at first because the sensor needs some time until it reaches the correct value. Then it oscillates and decreases a lot, probably because the sensor is not attached to the panel so it can freely move and sometimes it is in the shadows, which reduces a lot the radiation it perceives. So those values should not be interpreted like the radiation sank, because the modification of the radiation values are not proportional to the variations of the voltage values.

The voltage generated was not very high, maybe because the position was not the best because it was manually orientated. Moreover, the resistivity of the load was changed which explains the different values of the voltage even when the radiation is near $850\text{W}/\text{m}^2$. The angles remain

approximately stable because there were no great changes in the position, except the necessary modifications of the position to adjust the measurements. The temperature rises quickly because it was a hot and sunny day and the production of the power affects the temperature of the panel.

5.11. Measurement 11

In this measurement the conditions are the same, but it was started with the panel rotated 90° around the X-axis and then execute another rotation around the Y-axis. The voltage values are very small because of the rotation, since the panel is not facing the sun anymore and then is against the surface of the table (so the voltage is 0). The temperature even drops a little bit due to the lack of power generation. There is an important alteration of the values of the X-axis and the Z-axis when the rotation around the Y-axis takes place, which can be seen in Fig. 5.5.

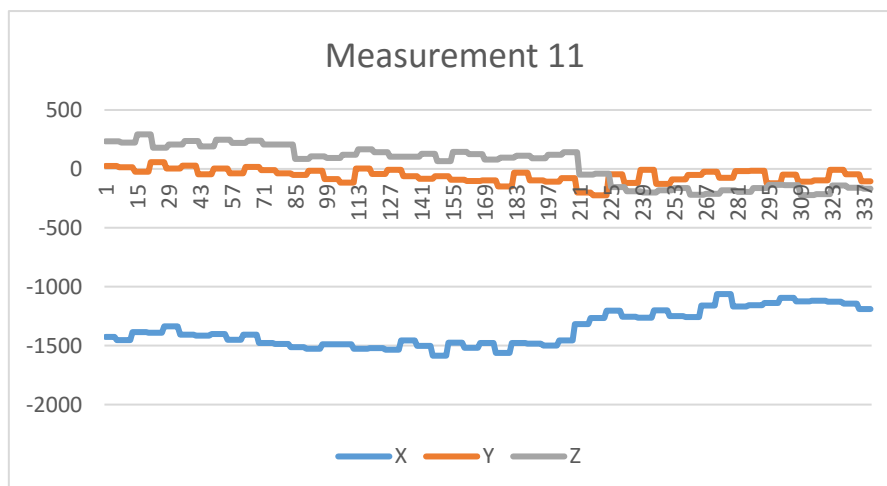


Fig. 5.5 Graphic created in Microsoft Excel® showing the results of Measurement 11

5.12. Measurement 12

In this case the current was checked, because the new circuit has been mounted with a silver wire as the shunt resistor. The experiment took place outside on a very sunny day, with radiation values that reach even 1000 W/m², in spite of the sensor moving afterwards and therefore getting low values. The changes in the voltage and current are due to the variable load, because the resistor was changed to check the circuit. Although the current values seem good, they did not coincide with the current values measured with a multimeter located after the load, connected in series with the current circuit. This may have been because the multimeter cables have an extra resistivity or because none of the current measuring methods is very precise. For this reason the current sensor was installed.

5.13. Measurement 13

For this measurement the new current sensor was already mounted, and the rest of the conditions remain the same as in the previous subsection. The change of the voltage and current values are again because the load was modified in order to get a wider range of results. When the current is negative, that does not imply that the current is flowing in the opposite direction. The meaning is that the voltage that drops on the sensor is smaller than the offset (2,35V) that must be subtracted in order to obtain the correct current values. Therefore, after this subtraction the result is negative and the current showed is negative. This can happen because the solar panel is generating a low power, or because the drop in the load is rather great and consequently the voltage that remains for the sensor is small. The temperature is rather high because the panel has been under the sun for some time and also producing energy, so it is very hot.

5.14. Measurement 14

The final experiment was a checking to make sure that everything was working properly. The conditions are the same as in the previous experiment. The solar panel was placed facing the sun, and it is possible to check that the voltage is very high now. Then a person stood up in front of it to see the effect of the shadow, and that is the reason why the voltage drop a little bit. This reduction is not so great because, as it was 10:00 in the morning, the sun was very high in the sky so the shadow was not directly in the panel but a little low. The radiation sensor was located next to the panel and also facing the sun, so the radiation values are proportional to the voltage. The angles remain stable because the solar panel was fixed to the table, so the only movements were when the table was moved a little bit while trying to adjust the circuit, the computer or some sensors. The current is very small because the load value was huge, so the drop of the voltage in the sensor is approximately the same as the subtracted offset.

6. CONCLUSION

Photovoltaic solar energy is one of the main renewable energies all over the world. The development of this energy source has contributed to the decrease of the average cost for producing electricity, and this cost is now very similar to the conventional energy sources cost. Furthermore, photovoltaic solar energy has still more scope for improvement, which means this cost can be reduced even more if the efficiency of the panels progresses.

It is then essential to show the future generations the importance of the renewable energies and especially of the photovoltaic solar energy. In order to do that, the universities have a fundamental role and must teach about those subjects. So this kind of initiatives, like the present thesis, are very important to show the working principles of this energy source and teach with practical lectures, which will help the students to better understand and retain the basic of the topic.

Nevertheless, it is important to perform the experiments properly during the practical lectures. The characterization of the solar panel will be done probably indoors due to the weather in this city, and then halogen lights will be used. Therefore, it is highly recommendable to follow the advice given in subsection 3.3.3 for the use of halogen lights for the characterization of solar panels. It is also essential to observe the "Manual of the program for the final user" in the subsection 4.9 in order to understand completely the functioning of the application and not execute any mistake, because the measurements can be compromised in that situation. It is especially critical to pay attention to the txt file where the data will be saved, to make sure it is empty and the user will not delete another measurement or will mix the data of two different experiments.

Furthermore, it is also vital to be careful with the electric circuit. As the solar panel generates a rather high voltage and current, it is imperative that always two people are working together in order to supervise each other's work. Moreover, it is fundamental to leave the panel disconnected until all the circuit is ready and checked. A good practice would be to locate the panel facing the table until everything is connected, later connect the panel, and then if everything is correct it is safe to orientate it towards the sun. This way the panel could not generate any current until it is connected, because it does not get any sunlight. So it is not dangerous to touch it because it is not producing electricity.

7. DISCUSSION OF THE RESULTS

The results of the different measurements have already been discussed in section 5. Concerning the thesis, the achieved results fulfil the objectives that were mentioned in section 1. The application for the measurement of the main characteristics of a photovoltaic solar module is complete, totally operative and it allows the user to save the data for a later analysis. It is also possible to send the data to other programs in order to perform mathematical operations or create graphics, as the V-I curve of the module.

The circuit with all the sensors that are necessary to measure this magnitudes is also designed and created. It senses all the desired magnitudes and accomplish other important requirements as the small size and light weight, which are essential for the assembly in the back of the solar panel.

An investigation about the spectrum of the light was also carried out. Upon the lecture of several scientific papers and the comparison between the results of their research, some conclusions were reached. Different artificial light sources were compared in order to find out the better source for the indoor characterization of solar panels, which will be the purpose of the practical lessons that will be hold. After the discovery that halogen light are the best sources, an analysis about the best way of characterising solar panels with those light was perform. Afterwards some recommendations were given in order to properly experiment with the halogen lights. Finally, a research about the degradation of the solar cells under the full light spectrum was made, in order to finish with a complete investigation about the spectrum of the light and the possible effects that it can have in the electricity generation.

Therefore, it is possible to say that all the objectives of the thesis have been achieved and that it is a successful work. Although there are still improvement possibilities, it is already possible to start working with the program and circuit because the application is fully functional.

8. SUMMARY AND PERSPECTIVES

The next step after this thesis should be the assembly of the circuit on the solar panel with PV tracker, because that panel is the one that will be used in the practical lectures next year and therefore the measurements should be made of this module. It is also important to correctly fix (with glue or another permanent fastening) the circuit, the temperature sensor and the radiation sensor. Although the circuit and the temperature sensor can be glued to the back of the panel, the radiation sensor must face in the same direction as the panel; so the best solution would be fix the sensor to one side of the panel and facing in the exact same direction to sit can sense the same radiation.

The following step should be trying to program the application on NI myRIO like it was planned, because NI myRIO allows wireless communication and consequently it would be possible to eliminate the USB cable between the circuit and the computer, because the information would be sent through a wireless network.

As a final improvement, it would be interesting to install the circuit into a box, because despite the cables being welded, it is safer to have the circuit close so no one can touch it or break it. Another amelioration could be the printing of the manual for the final user, along with a safety manual for a proper manipulation of the electrical devices.

9. BIBLIOGRAPHY

- EU ProSun. Energía solar mundial y de la UE. Retrieved from: <http://www.prosun.org/es/ue-solar-sostenible/energia-solar-mundial-y-de-la-ue.html>
- Lecue, A. (30th July 2011). Situación actual de la energía solar fotovoltaica en el mundo según el Plan de Energías Renovables PER 2011-2020. Retrieved from: <http://www.suelosolar.com/newsolares/newsol.asp?id=6209>
- Alternative Energy Tutorials (last updated July 2016). Solar Cell I-V Characteristic. Retrieved from: <http://www.alternative-energy-tutorials.com/energy-articles/solar-cell-i-v-characteristic.html>
- National Instruments. Retrieved from: <http://www.ni.com/es-es.html>
- Doutel, F. (18th August 2015). Guía del Arduinomaníaco: todo lo que necesitas saber sobre Arduino. Retrieved from: <http://www.xataka.com/especiales/guia-del-arduinomaniaco-todo-lo-que-necesitas-saber-sobre-arduino>
- Arduino. Retrieved from: <https://www.arduino.cc/>
- García, A. (9th January 2014). Aprendiendo a utilizar el sensor de temperatura DS18B20. Retrieved from: <https://panamahitek.com/aprendiendo-utilizar-el-sensor-de-temperatura-ds18b20/>
- Melexis. Triaxis[®] Micropower Magnetometer (Magnetic Field Sensor). Retrieved from: <https://www.melexis.com/en/product/MLX90393/Triaxis-Micropower-Magnetometer>
- Technische Alternative. Radiation sensor. Retrieved from: <http://www.ta.co.at/en/products/sensors/radiation-sensor.html>
- Allegro[™] MicroSystems, LLC. ACS712: Fully Integrated, Hall-Effect-Based Linear Current Sensor IC with 2.1 kVRMS Voltage Isolation and a Low-Resistance Current Conductor. Retrieved from: <http://www.allegromicro.com/en/Products/Current-Sensor-ICs/Zero-To-Fifty-Amp-Integrated-Conductor-Sensor-ICs/ACS712.aspx>
- PV Solar. Kyocera KC60, 60 Watt Solar Panel. Retrieved from: <http://www.pvsolar.com/kyocera/kc60.html>
- Böke, U., (2-5th September 2007). A simple model of photovoltaic module electric characteristics. *2007 European Conference on Power Electronics and Applications*, 1-8. Aalborg.
- Park, S. H., Ahn, S., Gwak, J., Shin, K., Ahn, S. K., Yoon, K., Cho, Y., Kim, D-W. and Yun, A.H. (October 2013). Effectiveness of full spectrum light soaking on solar cell degradation analysis. *Current Applied Physics*, Volume 13, 1684-1688.

Chapter 9: Bibliography

- Reyes-Rojas, W., Meza-Benavides, C. (2nd August 2014). Discusión y evaluación de fuentes de luz artificial para la caracterización de dispositivos fotovoltaicos. *Tecnología en Marcha, Edición especial Movilidad Estudiantil*, 31-40.
- Sepúlveda, S. (December 2014). Radiación solar: factor clave para el diseño de sistemas fotovoltaicos. *Revista MUNDO FESC, Volume 2 (8)*, 60-65.
- Minnaert, B. and Veelaert, P. (12th March 2014). A Proporsal for Typical Artificial Light Sources for the Characterization of Indoor Photovoltaic Applications. *Energies 2014, Volume 7*, 1500-1516.

10. APPENDIXES

10.1. Appendix 1: Results measurement 1

Date	Time	Voltage	Radiation	X axis	Y axis	Z axis	Current	Temperature
17.06.2016	12:38:04	18,478711	138,216561	-1438,000000	-33,000000	-46,000000	0,438965	25,000000
17.06.2016	12:38:04	18,478711	138,216561	-1438,000000	-33,000000	-46,000000	0,438965	24,000000
17.06.2016	12:38:05	18,983594	138,216561	-1438,000000	-33,000000	-46,000000	0,438965	24,000000
17.06.2016	12:38:05	18,983594	112,738854	-1438,000000	-33,000000	-46,000000	0,438965	24,000000
17.06.2016	12:38:05	18,983594	112,738854	-1411,000000	-33,000000	-46,000000	0,438965	24,000000
17.06.2016	12:38:05	18,983594	112,738854	-1411,000000	10,000000	-46,000000	0,438965	24,000000
17.06.2016	12:38:06	18,983594	112,738854	-1411,000000	10,000000	-48,000000	0,438965	24,000000
17.06.2016	12:38:06	18,983594	112,738854	-1411,000000	10,000000	-48,000000	0,438965	24,000000
17.06.2016	12:38:06	18,983594	112,738854	-1411,000000	10,000000	-48,000000	0,438965	24,000000
17.06.2016	12:38:07	18,983594	112,738854	-1411,000000	10,000000	-48,000000	0,438965	24,000000
17.06.2016	12:38:07	18,983594	125,477707	-1411,000000	10,000000	-48,000000	0,438965	24,000000
17.06.2016	12:38:07	18,983594	125,477707	-1453,000000	10,000000	-48,000000	0,438965	24,000000
17.06.2016	12:38:07	18,983594	125,477707	-1453,000000	-5,000000	-48,000000	0,438965	24,000000

Chapter 10: Appendixes

17.06.2016	12:38:07	18,983594	125,477707	-1453,000000	-5,000000	-9,000000	0,438965	24,000000
17.06.2016	12:38:08	18,983594	125,477707	-1453,000000	-5,000000	-9,000000	0,438965	24,000000
17.06.2016	12:38:08	18,983594	125,477707	-1453,000000	-5,000000	-9,000000	0,438965	24,000000
17.06.2016	12:38:08	18,983594	125,477707	-1453,000000	-5,000000	-9,000000	0,438965	24,000000
17.06.2016	12:38:09	18,983594	138,216561	-1453,000000	-5,000000	-9,000000	0,438965	24,000000
17.06.2016	12:38:09	18,983594	138,216561	-1416,000000	-5,000000	-9,000000	0,438965	24,000000
...								
17.06.2016	12:38:18	18,983594	125,477707	-1370,000000	95,000000	-89,000000	0,438965	25,000000
17.06.2016	12:38:18	18,983594	125,477707	-1370,000000	95,000000	-89,000000	0,438965	24,000000
17.06.2016	12:38:19	18,983594	125,477707	-1370,000000	95,000000	-89,000000	0,438965	24,000000
17.06.2016	12:38:19	18,983594	112,738854	-1370,000000	95,000000	-89,000000	0,438965	24,000000
17.06.2016	12:38:19	18,983594	112,738854	-1450,000000	95,000000	-89,000000	0,438965	24,000000
17.06.2016	12:38:19	18,983594	112,738854	-1450,000000	0,000000	-89,000000	0,438965	24,000000
17.06.2016	12:38:19	18,983594	112,738854	-1450,000000	0,000000	-56,000000	0,438965	24,000000
17.06.2016	12:38:20	18,983594	112,738854	-1450,000000	0,000000	-56,000000	0,438965	24,000000
17.06.2016	12:38:20	18,983594	112,738854	-1450,000000	0,000000	-56,000000	0,438965	25,000000
17.06.2016	12:38:20	18,983594	112,738854	-1450,000000	0,000000	-56,000000	0,438965	25,000000

10.2. Appendix 2: Results measurement 2

Date	Time	Voltage	Radiation	X axis	Y axis	Z axis	Current	Temperature
17.06.2016	12:43:16	19,942871	443,949045	-1401,000000	-2,000000	-37,000000	0,414551	32,000000
17.06.2016	12:43:16	19,942871	443,949045	-1401,000000	-2,000000	-37,000000	0,438477	32,000000
17.06.2016	12:43:16	19,942871	443,949045	-1401,000000	-2,000000	-37,000000	0,438477	34,000000
17.06.2016	12:43:17	18,529199	443,949045	-1401,000000	-2,000000	-37,000000	0,438477	34,000000
17.06.2016	12:43:17	18,529199	163,694268	-1401,000000	-2,000000	-37,000000	0,438477	34,000000
17.06.2016	12:43:17	18,529199	163,694268	-1451,000000	-2,000000	-37,000000	0,438477	34,000000
17.06.2016	12:43:17	18,529199	163,694268	-1451,000000	-11,000000	-37,000000	0,438477	34,000000
...								
17.06.2016	12:43:27	18,579688	176,433121	-1479,000000	-54,000000	-85,000000	0,438965	34,000000
17.06.2016	12:43:27	18,579688	176,433121	-1479,000000	-54,000000	-85,000000	0,438965	34,000000
17.06.2016	12:43:27	18,579688	176,433121	-1379,000000	-54,000000	-85,000000	0,438965	34,000000
17.06.2016	12:43:28	18,579688	176,433121	-1379,000000	-69,000000	-85,000000	0,438965	34,000000
17.06.2016	12:43:28	18,579688	176,433121	-1379,000000	-69,000000	-81,000000	0,438965	34,000000
17.06.2016	12:43:28	18,579688	176,433121	-1379,000000	-69,000000	-81,000000	0,438477	34,000000

10.3. Appendix 3: Results measurement 3

Date	Time	Voltage	Radiation	X axis	Y axis	Z axis	Current	Temperature
17.06.2016	12:39:46	19,791406	431,210191	-1442,000000	14,000000	-22,000000	0,438965	26,000000
17.06.2016	12:39:46	19,791406	431,210191	-1442,000000	14,000000	-22,000000	0,414551	26,000000
17.06.2016	12:39:46	19,791406	431,210191	-1442,000000	14,000000	-22,000000	0,414551	27,000000
17.06.2016	12:39:47	19,993359	431,210191	-1442,000000	14,000000	-22,000000	0,414551	27,000000
17.06.2016	12:39:47	19,993359	405,732484	-1442,000000	14,000000	-22,000000	0,414551	27,000000
17.06.2016	12:39:47	19,993359	405,732484	-1398,000000	14,000000	-22,000000	0,414551	27,000000
17.06.2016	12:39:47	19,993359	405,732484	-1398,000000	-85,000000	-22,000000	0,414551	27,000000
...								
17.06.2016	12:40:09	19,892383	418,471338	-1445,000000	1,000000	-87,000000	0,438965	27,000000
17.06.2016	12:40:09	19,892383	418,471338	-1413,000000	1,000000	-87,000000	0,438965	27,000000
17.06.2016	12:40:09	19,892383	418,471338	-1413,000000	-81,000000	-87,000000	0,438965	27,000000
17.06.2016	12:40:10	19,892383	418,471338	-1413,000000	-81,000000	-35,000000	0,438965	27,000000
17.06.2016	12:40:10	19,892383	418,471338	-1413,000000	-81,000000	-35,000000	0,438965	27,000000
17.06.2016	12:40:10	19,892383	418,471338	-1413,000000	-81,000000	-35,000000	0,438965	27,000000

10.4. Appendix 4: Results measurement 4

Date	Time	Voltage	Radiation	X axis	Y axis	Z axis	Current	Temperature
17.06.2016	12:41:42	19,892383	418,471338	-1413,000000	-81,000000	-35,000000	0,438965	27,000000
17.06.2016	12:41:42	19,993359	418,471338	-1413,000000	-81,000000	-35,000000	0,438965	27,000000
17.06.2016	12:41:42	19,993359	456,687898	-1381,000000	-81,000000	-35,000000	0,438965	27,000000
17.06.2016	12:41:43	19,993359	456,687898	-1381,000000	25,000000	-35,000000	0,438965	27,000000
17.06.2016	12:41:43	19,993359	456,687898	-1381,000000	25,000000	-94,000000	0,438965	27,000000
17.06.2016	12:41:43	19,993359	456,687898	-1381,000000	25,000000	-94,000000	0,438965	31,000000
17.06.2016	12:41:44	20,043848	456,687898	-1381,000000	25,000000	-94,000000	0,438965	31,000000
17.06.2016	12:41:44	20,043848	456,687898	-1381,000000	25,000000	-94,000000	0,438965	31,000000
...								
17.06.2016	12:42:03	19,892383	443,949045	-1401,000000	-77,000000	-74,000000	0,414062	32,000000
17.06.2016	12:42:03	19,892383	443,949045	-1401,000000	-2,000000	-74,000000	0,414062	32,000000
17.06.2016	12:42:03	19,892383	443,949045	-1401,000000	-2,000000	-37,000000	0,414062	32,000000
17.06.2016	12:42:04	19,892383	443,949045	-1401,000000	-2,000000	-37,000000	0,414551	32,000000
17.06.2016	12:42:04	19,892383	443,949045	-1401,000000	-2,000000	-37,000000	0,414551	32,000000

10.5. Appendix 5: Results measurement 5

Date	Time	Voltage	Radiation	X axis	Y axis	Z axis	Current	Temperature
17.06.2016	12:44:33	18,579688	176,433121	-1379,000000	-69,000000	-81,000000	0,438477	34,000000
17.06.2016	12:44:33	18,579688	176,433121	-1471,000000	-69,000000	-81,000000	0,438477	34,000000
17.06.2016	12:44:33	18,579688	176,433121	-1471,000000	-20,000000	-53,000000	0,438965	34,000000
17.06.2016	12:44:34	18,579688	176,433121	-1471,000000	-20,000000	-53,000000	0,438965	35,000000
17.06.2016	12:44:34	18,882617	176,433121	-1471,000000	-20,000000	-53,000000	0,438965	35,000000
17.06.2016	12:44:34	18,882617	227,388535	-1471,000000	-20,000000	-53,000000	0,438965	35,000000
17.06.2016	12:44:35	18,882617	227,388535	-1409,000000	-20,000000	-53,000000	0,438965	35,000000
17.06.2016	12:44:35	18,882617	227,388535	-1409,000000	6,000000	-17,000000	0,438965	35,000000
17.06.2016	12:44:35	18,882617	227,388535	-1409,000000	6,000000	-17,000000	0,438965	35,000000
17.06.2016	12:44:36	18,933105	227,388535	-1409,000000	6,000000	-17,000000	0,438965	35,000000
17.06.2016	12:44:36	18,933105	227,388535	-1409,000000	6,000000	-17,000000	0,438965	35,000000
17.06.2016	12:44:36	18,933105	227,388535	-1407,000000	-25,000000	-17,000000	0,438965	35,000000
17.06.2016	12:44:37	18,933105	227,388535	-1407,000000	-25,000000	-105,000000	0,438965	35,000000
17.06.2016	12:44:37	18,933105	227,388535	-1407,000000	-25,000000	-105,000000	0,438965	35,000000

17.06.2016	12:44:37	18,933105	227,388535	-1407,000000	-25,000000	-105,000000	0,438965	35,000000
17.06.2016	12:44:38	18,882617	227,388535	-1407,000000	-25,000000	-105,000000	0,438965	35,000000
17.06.2016	12:44:38	18,882617	227,388535	-1407,000000	-25,000000	-105,000000	0,438965	35,000000
17.06.2016	12:44:38	18,882617	227,388535	-1420,000000	37,000000	-105,000000	0,438965	35,000000
17.06.2016	12:44:38	18,882617	227,388535	-1420,000000	37,000000	-57,000000	0,438965	35,000000
17.06.2016	12:44:39	18,882617	227,388535	-1420,000000	37,000000	-57,000000	0,438965	35,000000
17.06.2016	12:44:39	18,882617	227,388535	-1420,000000	37,000000	-57,000000	0,438965	35,000000
17.06.2016	12:44:39	18,832129	227,388535	-1420,000000	37,000000	-57,000000	0,438965	35,000000
17.06.2016	12:44:40	18,832129	227,388535	-1420,000000	37,000000	-57,000000	0,438965	35,000000
17.06.2016	12:44:40	18,832129	227,388535	-1415,000000	37,000000	-57,000000	0,438965	35,000000
17.06.2016	12:44:40	18,832129	227,388535	-1415,000000	-28,000000	-92,000000	0,438965	35,000000
17.06.2016	12:44:40	18,832129	227,388535	-1415,000000	-28,000000	-92,000000	0,438965	35,000000
17.06.2016	12:44:41	18,832129	227,388535	-1415,000000	-28,000000	-92,000000	0,438965	35,000000
...								
17.06.2016	12:44:57	18,832129	227,388535	-1438,000000	-72,000000	-29,000000	0,438477	35,000000
17.06.2016	12:44:57	18,832129	227,388535	-1438,000000	-72,000000	-120,000000	0,438477	35,000000
17.06.2016	12:44:58	18,832129	227,388535	-1438,000000	-72,000000	-120,000000	0,438965	35,000000

10.6. Appendix 6: Results measurement 6

Date	Time	Voltage	Radiation	X axis	Y axis	Z axis	Current	Temperature
22.06.2016	12:15:35	0,000000	-1543,312102	0,000000	0,000000	0,000000	0,000000	0,000000
22.06.2016	12:15:36	0,706836	-1543,312102	0,000000	0,000000	0,000000	0,000000	0,000000
22.06.2016	12:15:37	0,706836	87,261146	0,000000	0,000000	0,000000	0,000000	0,000000
22.06.2016	12:15:37	0,706836	87,261146	-1052,000000	0,000000	0,000000	0,000000	0,000000
22.06.2016	12:15:37	0,706836	87,261146	-1052,000000	-17,000000	0,000000	0,000000	0,000000
22.06.2016	12:15:37	0,706836	87,261146	-1052,000000	-17,000000	46,000000	0,000000	0,000000
22.06.2016	12:15:37	0,706836	87,261146	-1052,000000	-17,000000	46,000000	1,129395	0,000000
...								
22.06.2016	12:15:58	0,706836	74,522293	-1092,000000	-3,000000	98,000000	1,129395	-127,000000
22.06.2016	12:15:58	0,706836	74,522293	-1092,000000	-3,000000	98,000000	1,129395	-127,000000
22.06.2016	12:15:58	0,706836	74,522293	-1092,000000	-3,000000	98,000000	1,129395	-127,000000
22.06.2016	12:15:59	0,656348	74,522293	-1092,000000	-3,000000	98,000000	1,129395	-127,000000
22.06.2016	12:15:59	0,656348	74,522293	-1092,000000	-3,000000	98,000000	1,129395	-127,000000
22.06.2016	12:15:59	0,656348	74,522293	-994,000000	-3,000000	98,000000	1,129395	-127,000000

10.7. Appendix 7: Results measurement 7

Date	Time	Voltage	Radiation	X axis	Y axis	Z axis	Current	Temperature
22.06.2016	12:17:00	0,656348	74,522293	-994,000000	40,000000	98,000000	1,129395	-127,000000
22.06.2016	12:17:00	0,656348	74,522293	-994,000000	40,000000	35,000000	1,129395	-127,000000
22.06.2016	12:17:01	0,656348	74,522293	-994,000000	40,000000	35,000000	1,129395	-127,000000
22.06.2016	12:17:01	0,656348	74,522293	-994,000000	40,000000	35,000000	1,129395	-127,000000
22.06.2016	12:17:01	0,605859	74,522293	-994,000000	40,000000	35,000000	1,129395	-127,000000
22.06.2016	12:17:02	0,605859	74,522293	-933,000000	40,000000	35,000000	1,129395	-127,000000
...								
22.06.2016	12:17:25	0,706836	74,522293	-956,000000	-58,000000	26,000000	1,129395	-127,000000
22.06.2016	12:17:25	0,706836	87,261146	-956,000000	-58,000000	26,000000	1,129395	-127,000000
22.06.2016	12:17:26	0,706836	87,261146	-987,000000	-58,000000	26,000000	1,129395	-127,000000
22.06.2016	12:17:26	0,706836	87,261146	-987,000000	-25,000000	26,000000	1,129395	-127,000000
22.06.2016	12:17:26	0,706836	87,261146	-987,000000	-25,000000	12,000000	1,129395	-127,000000
22.06.2016	12:17:26	0,706836	87,261146	-987,000000	-25,000000	12,000000	1,129395	-127,000000
22.06.2016	12:17:26	0,706836	87,261146	-987,000000	-25,000000	12,000000	1,129395	-127,000000

10.8. Appendix 8: Results measurement 8

Date	Time	Voltage	Radiation	X axis	Y axis	Z axis	Current	Temperature
22.06.2016	12:18:01	0,706836	87,261146	-987,000000	-25,000000	12,000000	1,129395	-127,000000
22.06.2016	12:18:01	0,706836	87,261146	-987,000000	-3,000000	12,000000	1,129395	-127,000000
22.06.2016	12:18:01	0,706836	87,261146	-987,000000	-3,000000	5,000000	1,129395	-127,000000
22.06.2016	12:18:02	0,706836	87,261146	-987,000000	-3,000000	5,000000	1,125000	-127,000000
22.06.2016	12:18:02	0,555371	87,261146	-987,000000	-3,000000	5,000000	1,125000	-127,000000
22.06.2016	12:18:02	0,555371	87,261146	-987,000000	-3,000000	5,000000	1,125000	-127,000000
...								
22.06.2016	12:18:23	0,706836	74,522293	-1006,000000	31,000000	43,000000	1,125000	-127,000000
22.06.2016	12:18:23	0,706836	74,522293	-948,000000	31,000000	43,000000	1,125000	-127,000000
22.06.2016	12:18:24	0,706836	74,522293	-948,000000	-3,000000	43,000000	1,125000	-127,000000
22.06.2016	12:18:24	0,706836	74,522293	-948,000000	-3,000000	-20,000000	1,125000	-127,000000
22.06.2016	12:18:24	0,706836	74,522293	-948,000000	-3,000000	-20,000000	1,129395	-127,000000
22.06.2016	12:18:24	0,706836	74,522293	-948,000000	-3,000000	-20,000000	1,129395	-127,000000
22.06.2016	12:18:25	0,757324	74,522293	-948,000000	-3,000000	-20,000000	1,129395	-127,000000

10.9. Appendix 9: Results measurement 9

Date	Time	Voltage	Radiation	X axis	Y axis	Z axis	Current	Temperature
22.06.2016	12:58:10	0,504883	87,261146	-1024,000000	0,000000	-72,000000	1,129395	-127,000000
22.06.2016	12:58:11	0,504883	87,261146	-1024,000000	-88,000000	-72,000000	1,129395	-127,000000
22.06.2016	12:58:11	0,504883	87,261146	-1024,000000	-88,000000	-44,000000	1,129395	-127,000000
22.06.2016	12:58:11	0,504883	87,261146	-1024,000000	-88,000000	-44,000000	1,129395	-127,000000
22.06.2016	12:58:12	0,555371	87,261146	-1024,000000	-88,000000	-44,000000	1,129395	-127,000000
22.06.2016	12:58:12	0,555371	87,261146	-1024,000000	-88,000000	-44,000000	1,129395	-127,000000
...								
22.06.2016	12:59:01	0,555371	74,522293	-998,000000	-6,000000	34,000000	1,129395	-127,000000
22.06.2016	12:59:01	0,555371	74,522293	-998,000000	-6,000000	34,000000	1,129395	-127,000000
22.06.2016	12:59:01	0,555371	74,522293	-998,000000	-6,000000	34,000000	1,129395	-127,000000
22.06.2016	12:59:02	0,555371	74,522293	-1014,000000	-6,000000	34,000000	1,129395	-127,000000
22.06.2016	12:59:02	0,555371	74,522293	-1014,000000	-17,000000	34,000000	1,129395	-127,000000
22.06.2016	12:59:02	0,555371	74,522293	-1014,000000	-17,000000	41,000000	1,129395	-127,000000
22.06.2016	12:59:02	0,555371	74,522293	-1014,000000	-17,000000	41,000000	1,129395	-127,000000

10.10. Appendix 10: Results measurement 10

Date	Time	Voltage	Radiation	X axis	Y axis	Z axis	Current	Temperature
20.06.2016	11:30:32	0,000000	-1543,312102	0,000000	0,000000	0,000000	0,000000	0,000000
20.06.2016	11:30:34	10,552051	-1543,312102	0,000000	0,000000	0,000000	0,000000	0,000000
20.06.2016	11:30:34	10,552051	851,592357	0,000000	0,000000	0,000000	0,000000	0,000000
20.06.2016	11:30:34	10,552051	851,592357	-1445,000000	0,000000	0,000000	0,000000	0,000000
20.06.2016	11:30:34	10,552051	851,592357	-1445,000000	-18,000000	0,000000	0,000000	0,000000
20.06.2016	11:30:34	10,552051	851,592357	-1445,000000	-18,000000	118,000000	0,000000	0,000000
20.06.2016	11:30:35	10,552051	851,592357	-1445,000000	-18,000000	118,000000	25,097656	0,000000
20.06.2016	11:30:35	10,552051	851,592357	-1445,000000	-18,000000	118,000000	25,097656	26,000000
20.06.2016	11:30:35	10,552051	851,592357	-1445,000000	-18,000000	118,000000	25,097656	26,000000
20.06.2016	11:30:36	10,552051	877,070064	-1445,000000	-18,000000	118,000000	25,097656	26,000000
...								
20.06.2016	11:30:52	10,451074	851,592357	-1422,000000	19,000000	213,000000	25,097656	26,000000
20.06.2016	11:30:52	10,451074	851,592357	-1422,000000	19,000000	213,000000	25,097656	26,000000
20.06.2016	11:30:53	10,451074	851,592357	-1422,000000	19,000000	213,000000	25,097656	26,000000

20.06.2016	11:30:53	10,451074	838,853503	-1422,000000	19,000000	213,000000	25,097656	26,000000
20.06.2016	11:30:53	10,451074	838,853503	-1397,000000	49,000000	213,000000	25,097656	26,000000
20.06.2016	11:30:53	10,451074	838,853503	-1397,000000	49,000000	222,000000	25,097656	26,000000
20.06.2016	11:30:54	10,451074	838,853503	-1397,000000	49,000000	222,000000	25,195312	26,000000
20.06.2016	11:30:54	10,451074	838,853503	-1397,000000	49,000000	222,000000	25,195312	25,000000
20.06.2016	11:30:54	10,451074	838,853503	-1397,000000	49,000000	222,000000	25,195312	25,000000
...								
20.06.2016	11:42:11	0,151465	392,993631	-1412,000000	33,000000	275,000000	25,878906	29,000000
20.06.2016	11:42:11	0,151465	392,993631	-1412,000000	33,000000	275,000000	25,878906	29,000000
20.06.2016	11:42:11	0,151465	392,993631	-1412,000000	33,000000	275,000000	25,878906	29,000000
20.06.2016	11:42:12	0,151465	392,993631	-1397,000000	33,000000	275,000000	25,878906	29,000000
20.06.2016	11:42:12	0,151465	392,993631	-1397,000000	26,000000	275,000000	25,878906	29,000000
20.06.2016	11:42:12	0,151465	392,993631	-1397,000000	26,000000	235,000000	25,878906	29,000000
20.06.2016	11:42:12	0,151465	392,993631	-1397,000000	26,000000	235,000000	25,878906	29,000000
20.06.2016	11:42:12	0,151465	392,993631	-1397,000000	26,000000	235,000000	25,878906	29,000000
20.06.2016	11:42:13	0,151465	392,993631	-1397,000000	26,000000	235,000000	25,878906	29,000000
20.06.2016	11:42:13	0,151465	380,254777	-1397,000000	26,000000	235,000000	25,878906	29,000000

10.11. Appendix 11: Results measurement 11

Date	Time	Voltage	Radiation	X axis	Y axis	Z axis	Current	Temperature
20.06.2016	11:42:50	0,151465	380,254777	-1426,000000	26,000000	235,000000	25,878906	29,000000
20.06.2016	11:42:50	0,151465	380,254777	-1426,000000	26,000000	235,000000	25,976562	29,000000
20.06.2016	11:42:50	0,151465	380,254777	-1426,000000	26,000000	235,000000	25,976562	29,000000
20.06.2016	11:42:51	0,151465	380,254777	-1426,000000	26,000000	235,000000	25,976562	29,000000
20.06.2016	11:42:51	0,151465	392,993631	-1426,000000	26,000000	235,000000	25,976562	29,000000
20.06.2016	11:42:51	0,151465	392,993631	-1453,000000	26,000000	235,000000	25,976562	29,000000
20.06.2016	11:42:51	0,151465	392,993631	-1453,000000	14,000000	235,000000	25,976562	29,000000
...								
20.06.2016	11:44:12	0,000000	303,821656	-1190,000000	-45,000000	-161,000000	25,097656	28,000000
20.06.2016	11:44:12	0,000000	303,821656	-1190,000000	-105,000000	-161,000000	25,097656	28,000000
20.06.2016	11:44:13	0,000000	303,821656	-1190,000000	-105,000000	-167,000000	25,097656	28,000000
20.06.2016	11:44:13	0,000000	303,821656	-1190,000000	-105,000000	-167,000000	25,097656	28,000000
20.06.2016	11:44:13	0,000000	303,821656	-1190,000000	-105,000000	-167,000000	25,097656	29,000000
20.06.2016	11:44:13	0,000000	303,821656	-1190,000000	-105,000000	-167,000000	25,097656	29,000000

10.12. Appendix 12: Results measurement 12

Date	Time	Voltage	Radiation	X axis	Y axis	Z axis	Current	Temperature
23.06.2016	09:07:50	0,000000	-1543,312102	0,000000	0,000000	0,000000	0,000000	0,000000
23.06.2016	09:07:52	0,605859	-1543,312102	0,000000	0,000000	0,000000	0,000000	0,000000
23.06.2016	09:07:52	0,605859	609,554140	0,000000	0,000000	0,000000	0,000000	0,000000
23.06.2016	09:07:53	0,605859	609,554140	-1243,000000	0,000000	0,000000	0,000000	0,000000
23.06.2016	09:07:53	0,605859	609,554140	-1243,000000	-114,000000	0,000000	0,000000	0,000000
23.06.2016	09:07:53	0,605859	609,554140	-1243,000000	-114,000000	-98,000000	0,000000	0,000000
23.06.2016	09:07:53	0,605859	609,554140	-1243,000000	-114,000000	-98,000000	1,120605	0,000000
23.06.2016	09:07:53	0,605859	609,554140	-1243,000000	-114,000000	-98,000000	1,120605	32,000000
...								
23.06.2016	09:22:11	10,400586	596,815287	-1100,000000	-79,000000	35,000000	1,133789	39,000000
23.06.2016	09:22:12	10,400586	596,815287	-1116,000000	-79,000000	35,000000	1,133789	39,000000
23.06.2016	09:22:12	10,400586	596,815287	-1116,000000	-87,000000	35,000000	1,133789	39,000000
23.06.2016	09:22:12	10,400586	596,815287	-1116,000000	-87,000000	39,000000	1,133789	39,000000
23.06.2016	09:22:14	10,400586	596,815287	-1116,000000	-87,000000	39,000000	1,133789	39,000000

10.13. Appendix 13: Results measurement 13

Date	Time	Voltage	Radiation	X axis	Y axis	Z axis	Current	Temperature
23.06.2016	09:54:38	0,000000	-1543,312102	0,000000	0,000000	0,000000	-12,702700	0,000000
23.06.2016	09:54:38	0,000000	-1543,312102	-1093,000000	0,000000	0,000000	-12,702700	0,000000
23.06.2016	09:54:38	0,000000	-1543,312102	-1093,000000	-82,000000	0,000000	-12,702700	0,000000
23.06.2016	09:54:38	0,000000	-1543,312102	-1093,000000	-82,000000	40,000000	-12,702700	0,000000
23.06.2016	09:54:38	0,000000	-1543,312102	-1093,000000	-82,000000	40,000000	0,124053	0,000000
23.06.2016	09:54:39	0,000000	-1543,312102	-1093,000000	-82,000000	40,000000	0,124053	43,000000
23.06.2016	09:54:40	10,854980	-1543,312102	-1093,000000	-82,000000	40,000000	0,124053	43,000000
23.06.2016	09:54:40	10,854980	112,738854	-1093,000000	-82,000000	40,000000	0,124053	43,000000
23.06.2016	09:54:40	10,854980	112,738854	-1119,000000	-82,000000	40,000000	0,124053	43,000000
23.06.2016	09:54:40	10,854980	112,738854	-1119,000000	-108,000000	40,000000	0,124053	43,000000
...								
23.06.2016	09:54:52	10,804492	112,738854	-1088,000000	-57,000000	41,000000	-0,148857	43,000000
23.06.2016	09:54:52	10,804492	112,738854	-1088,000000	-57,000000	41,000000	-0,148857	43,000000
23.06.2016	09:54:53	10,400586	112,738854	-1088,000000	-57,000000	41,000000	-0,148857	43,000000

23.06.2016	09:54:54	10,400586	112,738854	-1088,000000	-57,000000	41,000000	-0,148857	43,000000
23.06.2016	09:54:54	10,400586	112,738854	-1065,000000	-57,000000	41,000000	-0,148857	43,000000
23.06.2016	09:54:54	10,400586	112,738854	-1065,000000	-130,000000	41,000000	-0,148857	43,000000
23.06.2016	09:54:54	10,400586	112,738854	-1065,000000	-130,000000	23,000000	-0,148857	43,000000
23.06.2016	09:54:54	10,400586	112,738854	-1065,000000	-130,000000	23,000000	-0,024807	43,000000
23.06.2016	09:54:55	10,400586	112,738854	-1065,000000	-130,000000	23,000000	-0,024807	43,000000
23.06.2016	09:54:56	10,501563	112,738854	-1065,000000	-130,000000	23,000000	-0,024807	43,000000
...								
23.06.2016	09:57:43	16,661133	125,477707	-1059,000000	-97,000000	74,000000	1,414171	42,000000
23.06.2016	09:57:44	16,661133	125,477707	-1059,000000	-97,000000	74,000000	1,414171	42,000000
23.06.2016	09:57:45	16,661133	125,477707	-1059,000000	-97,000000	74,000000	1,414171	42,000000
23.06.2016	09:57:45	16,661133	125,477707	-1059,000000	-97,000000	74,000000	1,414171	42,000000
23.06.2016	09:57:45	16,661133	125,477707	-1060,000000	-97,000000	74,000000	1,414171	42,000000
23.06.2016	09:57:45	16,661133	125,477707	-1060,000000	-61,000000	74,000000	1,414171	42,000000
23.06.2016	09:57:45	16,661133	125,477707	-1060,000000	-61,000000	23,000000	1,414171	42,000000
23.06.2016	09:57:46	16,661133	125,477707	-1060,000000	-61,000000	23,000000	1,240501	42,000000
23.06.2016	09:57:46	16,661133	125,477707	-1060,000000	-61,000000	23,000000	1,240501	42,000000

Chapter 10: Appendixes

23.06.2016	09:57:47	16,711621	125,477707	-1060,000000	-61,000000	23,000000	1,240501	42,000000
...								
23.06.2016	10:01:25	18,125293	112,738854	-1064,000000	-88,000000	68,000000	0,570632	42,000000
23.06.2016	10:01:25	18,125293	112,738854	-1064,000000	-88,000000	68,000000	0,570632	42,000000
23.06.2016	10:01:26	18,125293	112,738854	-1064,000000	-88,000000	68,000000	0,570632	42,000000
23.06.2016	10:01:27	18,125293	112,738854	-1064,000000	-88,000000	68,000000	0,570632	42,000000
23.06.2016	10:01:27	18,125293	112,738854	-1051,000000	-88,000000	68,000000	0,570632	42,000000
23.06.2016	10:01:27	18,125293	112,738854	-1051,000000	-158,000000	68,000000	0,570632	42,000000
23.06.2016	10:01:27	18,125293	112,738854	-1051,000000	-158,000000	7,000000	0,570632	42,000000
23.06.2016	10:01:27	18,125293	112,738854	-1051,000000	-158,000000	7,000000	0,719492	42,000000
23.06.2016	10:01:28	18,125293	112,738854	-1051,000000	-158,000000	7,000000	0,719492	42,000000
23.06.2016	10:01:29	18,125293	112,738854	-1051,000000	-158,000000	7,000000	0,719492	42,000000

10.14. Appendix 14: Results measurement 14

Date	Time	Voltage	Radiation	X axis	Y axis	Z axis	Current	Temperature
23.06.2016	10:04:51	19,236035	1017,197452	-1025,000000	-89,000000	73,000000	-0,049617	42,000000
23.06.2016	10:04:52	19,236035	1017,197452	-1025,000000	-89,000000	73,000000	-0,049617	42,000000
23.06.2016	10:04:52	19,236035	1004,458599	-1025,000000	-89,000000	73,000000	-0,049617	42,000000
23.06.2016	10:04:52	19,236035	1004,458599	-1074,000000	-89,000000	73,000000	-0,049617	42,000000
23.06.2016	10:04:53	19,236035	1004,458599	-1074,000000	-83,000000	73,000000	-0,049617	42,000000
23.06.2016	10:04:53	19,236035	1004,458599	-1074,000000	-83,000000	55,000000	-0,049617	42,000000
23.06.2016	10:04:53	19,236035	1004,458599	-1074,000000	-83,000000	55,000000	-0,148857	42,000000
23.06.2016	10:04:53	19,236035	1004,458599	-1074,000000	-83,000000	55,000000	-0,148857	42,000000
23.06.2016	10:04:54	19,236035	1004,458599	-1074,000000	-83,000000	55,000000	-0,148857	42,000000
23.06.2016	10:04:54	19,236035	1004,458599	-1074,000000	-83,000000	55,000000	-0,148857	42,000000
...								
23.06.2016	10:05:30	17,822363	978,980892	-1076,000000	-82,000000	94,000000	0,000003	42,000000
23.06.2016	10:05:31	17,721387	978,980892	-1076,000000	-82,000000	94,000000	0,000003	42,000000
23.06.2016	10:05:31	17,721387	966,242038	-1076,000000	-82,000000	94,000000	0,000003	42,000000

Chapter 10: Appendixes

23.06.2016	10:05:31	17,721387	966,242038	-1032,000000	-82,000000	94,000000	0,000003	42,000000
23.06.2016	10:05:32	17,721387	966,242038	-1032,000000	-62,000000	89,000000	0,000003	42,000000
23.06.2016	10:05:32	17,721387	966,242038	-1032,000000	-62,000000	89,000000	0,148862	42,000000
23.06.2016	10:05:32	17,721387	966,242038	-1032,000000	-62,000000	89,000000	0,148862	42,000000
23.06.2016	10:05:33	18,125293	966,242038	-1032,000000	-62,000000	89,000000	0,148862	42,000000
23.06.2016	10:05:33	18,125293	966,242038	-1032,000000	-62,000000	89,000000	0,148862	42,000000
...								
23.06.2016	10:05:45	19,337012	1017,197452	-1127,000000	-116,000000	46,000000	-0,248097	42,000000
23.06.2016	10:05:46	19,337012	1017,197452	-1127,000000	-116,000000	46,000000	-0,248097	42,000000
23.06.2016	10:05:47	19,286523	1017,197452	-1127,000000	-116,000000	46,000000	-0,248097	42,000000
23.06.2016	10:05:47	19,286523	1017,197452	-1127,000000	-116,000000	46,000000	-0,248097	42,000000
23.06.2016	10:05:47	19,286523	1017,197452	-1038,000000	-116,000000	46,000000	-0,248097	42,000000
23.06.2016	10:05:47	19,286523	1017,197452	-1038,000000	-133,000000	46,000000	-0,248097	42,000000
23.06.2016	10:05:48	19,286523	1017,197452	-1038,000000	-133,000000	35,000000	-0,248097	42,000000
23.06.2016	10:05:48	19,286523	1017,197452	-1038,000000	-133,000000	35,000000	-0,223287	42,000000
23.06.2016	10:05:48	19,286523	1017,197452	-1038,000000	-133,000000	35,000000	-0,223287	42,000000
23.06.2016	10:05:49	19,286523	1017,197452	-1038,000000	-133,000000	35,000000	-0,223287	42,000000